



**TRIBHUVAN UNIVERSITY
INSTITUTE OF ENGINEERING
PULCHOWK CAMPUS**

**Performance Evaluation of MIMO-OFDM System by PAPR
Reduction and Channel Estimation**

By

Hariom Dhungana

(066/MSICE/607)

A thesis

Submitted in partial fulfillment of the requirement for the degree
of Master of Science in Information and Communication
Engineering

Masters of Science in Information and Communication
Engineering Committee,
Department of Electronics and Computer Engineering

Oct, 2011

**Performance Evaluation of MIMO-OFDM System by PAPR
Reduction and Channel Estimation**

Copyright

The author has agreed that the library, Department of Electronics and Computer Engineering, Institute of Engineering, Pulchowk Campus, may make this thesis freely available for inspection. Moreover the author has agreed that the permission for extensive copying of this thesis work for scholarly purpose may be granted by the professors, who supervised the thesis work recorded herein or, in their absence, by the Head of the Department, wherein this thesis was done. It is understood that the recognition will be given to the author of this thesis and to the Department of Electronics and Computer Engineering, Pulchowk Campus in any use of the material of this thesis. Copying of publication or other use of this thesis for financial gain without approval of the Department of Electronics and Computer Engineering, Pulchowk Campus, Institute of Engineering and author's written permission is prohibited. Request for permission to copy or to make any use of the material in this thesis in whole or part should be addressed to:

Head
Department of Electronics and Computer Engineering
Pulchowk Campus
Institute of Engineering
Lalitpur, Nepal

Abstract

There are not limit of human desire so day by day we need much higher data speed to facilitate our need but every physical resources like frequency band, transmit signal strength are finite. Within the given limited resource higher data speed is accomplished by new proficiency called Multiple Input Multiple Output (MIMO), Orthogonal Frequency Division Multiplexing (OFDM) system. MIMO-OFDM fulfills the high data rate requirement through spatial multiplexing gain and improved link reliability due to antenna diversity gain. With this technique both interference reduction and maximum diversity gain are achieved by increasing number of antennas on either side.

Performance of MIMO-OFDM system depends on various factors like channel characteristics, SNR, fading, etc. Among them peak to average power ratio (PAPR) and channel estimation are major parameters that must be primarily addressed. In the thesis various PAPR determining factors such as no of subcarriers, oversampling rate and modulation scheme are studied and their effects are analyzed. Clipping, coding, symbol scrambling, adaptive predistortion and DFT-spreading technique for PAPR reduction are thoroughly discussed. Furthermore, comparison among their characteristics is simulated in MATLAB and useful conclusion is delineated.

Received signal in MIMO-OFDM system usually distorted by multipath fading. In order to recover the transmitted signal correctly, channel effect must be estimated and repaired at receiver. In the thesis several channel estimation method are mediated and appropriate solution is recommended. To relieve from overhead of training symbols, which significantly shrink the system bandwidth-efficiency, blind channel estimation algorithm is compared with training based channel estimation technique.

Acknowledgement

This is my pleasure to submit the thesis report on “**Performance Evaluation of MIMO-OFDM System by PAPR Reduction and Channel Estimation**” to department of Electronics and Computer Engineering for the partial fulfillment of the requirements for the degree of Masters of Science in Information and Communication Engineering.

First and foremost I would like to express my gratitude to Prof. Dinesh Kumar Sharma, PhD my thesis supervisor, for his invaluable advice, kind support and encouragement.

My sincere thanks to Prof. Shashidhar Ram Joshi, Head of Department of Electronics and Computer Engineering; Asst. Prof. Sarad Kumar Ghimire, M. Sc Program Coordinator, for giving me the opportunity to carry out this thesis, guidance and help me in many ways. Words are inadequate in offering my thanks to my respected teachers of MSICE Committee and my friends for their encouraged and cooperation in carrying out the thesis.

Above all; my complete heartfelt and utmost thanks to my beloved parents for their blessings, support and wishes for the successful completion of this thesis.

Hariom Dhungana

(066/MSICE/607)

Contents

Copyright	iii
Abstract	iv
Acknowledgement	v
Contents.....	vi
List of Figures	ix
List of Tables.....	xi
Abbreviations	xii
1 Introduction	1
1.1 Common research matter	2
1.2 Thesis objective	2
1.3 Organization of thesis.....	3
2 Wireless Channel Model.....	4
2.1 Path loss	6
2.2 Fading.....	7
3 Multiple Input Multiple Output (MIMO)	9
3.1 Background	9
3.2 MIMO Channel Capacity	9
3.2.1 Spatial Multiplexing	10
3.2.2 Diversity Coding.....	11
3.2.3 Precoding	12
4 Orthogonal Frequency Division Multiplexing (OFDM)	13
4.1 Introduction	13
4.2 Cyclic Prefix.....	17
4.3 The Peak to Average Power Ratio	18
4.4 PAPR Determining Elements	19
4.4.1 Number of sub-carriers.....	19

4.4.2	Oversampling rate	20
4.4.3	Modulation Schemes	21
4.5	PAPR Reduction Technique.....	22
4.5.1	Signal distortion techniques (clipping, peak windowing, peak cancellation)	24
4.5.2	Coding techniques	26
4.5.3	Symbol scrambling.....	27
4.5.4	Adaptive Predistortion Technique.....	32
4.5.5	DFT-spreading Technique	32
5	Channel Estimation.....	35
5.1	Background	35
5.2	Pilot Structure	36
5.3	Training Symbol Based Channel Estimation	38
5.3.1	Least Square Channel Estimation	38
5.3.2	Minimum Mean Square Error Channel Estimation	39
5.4	Processing Domain Estimation.....	40
5.5	Iteration versus Direct channel estimation	40
5.6	DFT-Based Channel Estimation.....	40
5.7	Advanced Channel Estimation Technique.....	42
5.7.1	Blind channel estimation technique	42
6	Simulation and Result	46
6.1	PAPR characteristics in SLM	46
6.2	PAPR characteristics in PTS	48
6.3	Comparison between SLM and PTS algorithm	49
6.3.1	Auxiliary information comparison	49
6.3.2	Caparison of PAPR reduction performance between SLM and PTS	50
6.4	PAPR characteristic in DFT-spreading technique	51
6.5	Bit Error Rate in MIMO	55

6.6 Comparison of LS and MMSE Estimator	56
6.7 DFT Based Channel Estimation.....	59
6.8 NRMSE simulation for blind channel estimation	61
7 Conclusions and Future works	63
7.1 Conclusions.....	63
7.2 Future works	65
Reference:	66
Appendices.....	69
1 Flow chart of SLM (left) and PTS (right).....	69
2 PAPR reduction comparison between SLM and PTS method	70

List of Figures

Fig 1 Channel Classification: Propagation, Radio, Modulation and Digital Channel....	5
Fig 2 Spatially multiplexed MIMO systems	11
Fig 3 Concept of the OFDM signal: (a) conventional multicarrier technique, and (b) orthogonal multicarrier modulation technique	14
Fig 4 Spectra of (a) an OFDM sub channel, and (b) an OFDM signal	15
Fig 5 A Digital Implementation of a Baseband OFDM System	16
Fig 6 OFDM symbols with CP.....	17
Fig 7 PAPR performance with different values of subcarriers	20
Fig 8 PAPR performance with different values of oversampling rate	21
Fig 9 PAPR performance with various modulation schemes	22
Fig 10 Block diagram of a PAPR reduction scheme using clipping and filtering	25
Fig 11 Block diagram of selective mapping (SLM) technique for PAPR reduction ...	28
Fig 12 Block diagram of partial transmit sequence technique	30
Fig 13 Equivalence of OFDMA system with DFT-spreading code to a single-carrier system	33
Fig 14 Examples of DFT spreading for IFDMA, DFDMA and LFDMA: three users with $N=12$; $M= 4$	34
Fig 15 Block diagram of channel estimation	35
Fig 16 OFDM system with pilot based channel estimation.....	37
Fig 17 DFT-Based Channel Estimation.....	41
Fig 18 MIMO-OFDM system model with M_t transmit and M_r receive antennas	44
Fig 19 PAPR reduction performances with a) different values of route number with subcarrier $N=128$ b) different values of subcarrier with route number $M=8$	47
Fig 20 PAPR reduction performances with a) different values of no of subblocks V b) different values of no of allowed phase factors W	48
Fig 21 PAPR reduction performances with different subblocks partition schemes	48
Fig 22 Comparison of PAPR reduction performances between PTS algorithm and SLM algorithm for MIMO-OFDM system.....	51
Fig 23 PAPR performances of DFT-spreading technique for IFDMA, LFDMA, and OFDMA	52
Fig 24 PAPR performances of DFT-spreading technique with pulse shaping	52
Fig 25 PAPR performance of DFT-spreading for variable subcarrier	53
Fig 26 Bit error rate for various antenna arrangements.....	55
Fig 27 Mean Square Error comparison for LS and MMSE estimator.....	58
Fig 28 Symbol Error Rate comparison for LS and MMSE estimator	58
Fig 29 Constellation diagram of received signal.....	59

Fig 30 Comparison with and without DFT-Based channel estimation 60
Fig 31 Comparison of NRMSE performance vs SNR (left) and no of OFDM symbols
(right) 62

List of Tables

Table 1 Comparison effects of PAPR reduction technique	34
Table 2 SLM and PTS Comparison with different M V values.....	50
Table 3 LS and MMSE comparison	57

Abbreviations

MIMO	Multiple Input Multiple Output
OFDM	Orthogonal Frequency Division Multiplexing
CSI	Channel State Information
DFT	Discrete Fourier Transform
IDFT	Inverse Discrete Fourier Transform
FFT	Fast Fourier Transform
IFFT	Inverse Fast Fourier Transform
ADC	Analog to Digital Converter
CP	Cyclic Prefix
VC	Virtual Carrier
SC	Sub Carrier
ISI	Inter Symbol Interference
SVD	Singular Value Decomposition
QoS	Quality of Service
MSE	Mean Square Error
NRMSE	Normalized Root Mean Square Error
LS	Least square
MMSE	Minimum Mean Square Error
SLM	Selective Mapping
PTS	Partial Transmit Sequence
SNR	Signal to Noise Ratio
BER	Bit Error Rate
CDF	Cumulative Distributive Function

1 Introduction

During the past decades, wireless communication has benefitted from substantial advances and it is considered as the key enabling technique of innovative future consumer products. For the sake of satisfying the requirements of various applications, significant technological achievements are required to ensure that wireless devices have appropriate architectures suitable for supporting a wide range of services delivered to the users. In the foreseeable future, the large-scale deployment of wireless devices and the requirements of high bandwidth applications are expected to lead to tremendous new challenges in terms of the efficient exploitation of the achievable spectral resources [1]. Among the existing air-interface techniques, orthogonal frequency division multiplexing (OFDM) has shown a number of advantages and has attracted substantial interest. OFDM converts a frequency-selective channel into a parallel collection of frequency flat sub channels. The subcarriers have the minimum frequency separation required to maintain orthogonality of their corresponding time domain waveforms, yet the signal spectra corresponding to the different subcarriers overlap in frequency. Hence, the available bandwidth is very efficiently used [2]. If knowledge of the channel is available at the transmitter, then the OFDM transmitter can adapt its signaling strategy to match the channel. Due to the fact that OFDM uses a large collection of narrowly spaced sub channels, these adaptive strategies can approach the ideal water pouring capacity of a frequency-selective channel [3]. In practice this is achieved by using adaptive bit loading techniques, where different sized signal constellations are transmitted on the subcarriers.

With a drastic increase in number of users feeling comfortable while accessing wireless services in last few years, there is a fair demand for higher system throughputs to accommodate more users with higher data rates. It is illustrious that MIMO based OFDM has the potential to achieve high system capacity and transmit-receive diversity for reliable communication links of any wireless system, hence it is considered as the future of wireless communication systems [1]. MIMO OFDM

systems provide higher data rates, support a large number of users with flexibility in Quality of Service (QoS) and provide high quality transmission in comparison to other schemes. But in order to fulfill these requirements some constraints have to be very well addressed such as limited availability of frequency spectrum, availability of total transmit power and nature of wireless channels [4].

1.1 Common research matter

MIMO-OFDM system has different diversified field of research matter. Common challenging issues are System capacity, which cumulate overall performances. Efficient coding scheme is always welcomed in wireless communication and Space/Time/Frequency coding is also hot cake in present scenario. Power is worthy parameter and saving the power is overt topic, precoding and minimization of power consumption by communicating device are also vital issues. Multicarrier system suffers from peak to average power problem and synchronization of OFDM signal is also critical subject. There are a lot of jobs for researcher. From these bountiful liabilities this thesis has chosen the analysis of peak to average power ratio minimization technique and channel estimation.

1.2 Thesis objective

Peak to average power ratio (PAPR) being a inevitable random variable in multicarrier system, but can be minimize by different technique. An appropriate description of PAPR is its complementary cumulative distribution function (CCDF). In this report different PAPR reduction techniques are analyzed based on the characteristics of CCDF. Another objective of this thesis is to present efficient channel estimation technique. The bit error rate mean square error and symbol error rate are performance evaluating parameter in channel estimation. On the basis of the required accuracy of the estimate and optimal training sequences of minimum length, channel estimators are chosen.

1.3 Organization of thesis

This thesis begins from the introduction of current wireless communication pattern, objective of thesis followed by organization of thesis. Chapter 2 presents the wireless channel model followed by path loss and fading. Chapter 3 includes the MIMO channel pursued by system attributes like spatial multiplexing, diversity coding and precoding. Next chapter describes the OFDM system & its various aspects, furthermore diverse PAPR reduction techniques are studied. Chapter 4 confines the channel estimation method in MIMO-OFDM system. Chapter 6 includes system model and simulation of PAPR reduction technique and comparison of Least Square Channel Estimation and minimum mean square error channel estimation method. Statements are resolved on the basis of simulation result. Finally conclusions are drawn from simulation result and wrap up the thesis drawing by giving some implication, future works for further research and recommendations.

2 Wireless Channel Model

The performance of any communication system is primarily decided by the communication channel. There are different types of channels among them wireless channel has unreliable behavior; the state of the channel may change within a very short time span. This stochastic and rapid behavior of radio channels turns wireless data communication into a difficult task. In this chapter I want to focus on the factors which influence the performance of wireless channels. Wireless channel in a communication system are categorized into four types according to the different instances in the transmission and reception process of signal [14].

The first one is propagation channel, which confines between the transmitter and receiver antennas. It is almost linear, reciprocal and attenuation of the transmitted signal has multiplicative effect on the signal. The signal transmitted consists of the information modulated on top of the carrier frequency. The second one, radio channel, includes the propagation channel and both of the antennas on each side transmitting and receiving end. As long as the antennas are considered to be linear, bilateral and passive, the channel is also linear and reciprocal. The third type, modulation channel, consists of the radio channel plus all system components (like amplifiers and different stages of radio frequency circuits) up to the output of the modulator on the transmitter side and the input of the demodulator on the receiver side. The characteristics of channel depend on the transfer function of the components like amplifiers, antennas. The signal consists here of the baseband symbols. The final type, digital channel, covers the modulation channel plus the modulator and demodulator. It connects the digital baseband signal at the transmitter to the digital signal at the receiver via the bit patterns. The bits are grouped then and turned into analog representations, so called symbols. Due to the nonlinear module fused with the channel its characteristic is non-linear and non-reciprocal. Pictorial view of all channel type is depicted in Fig 1.

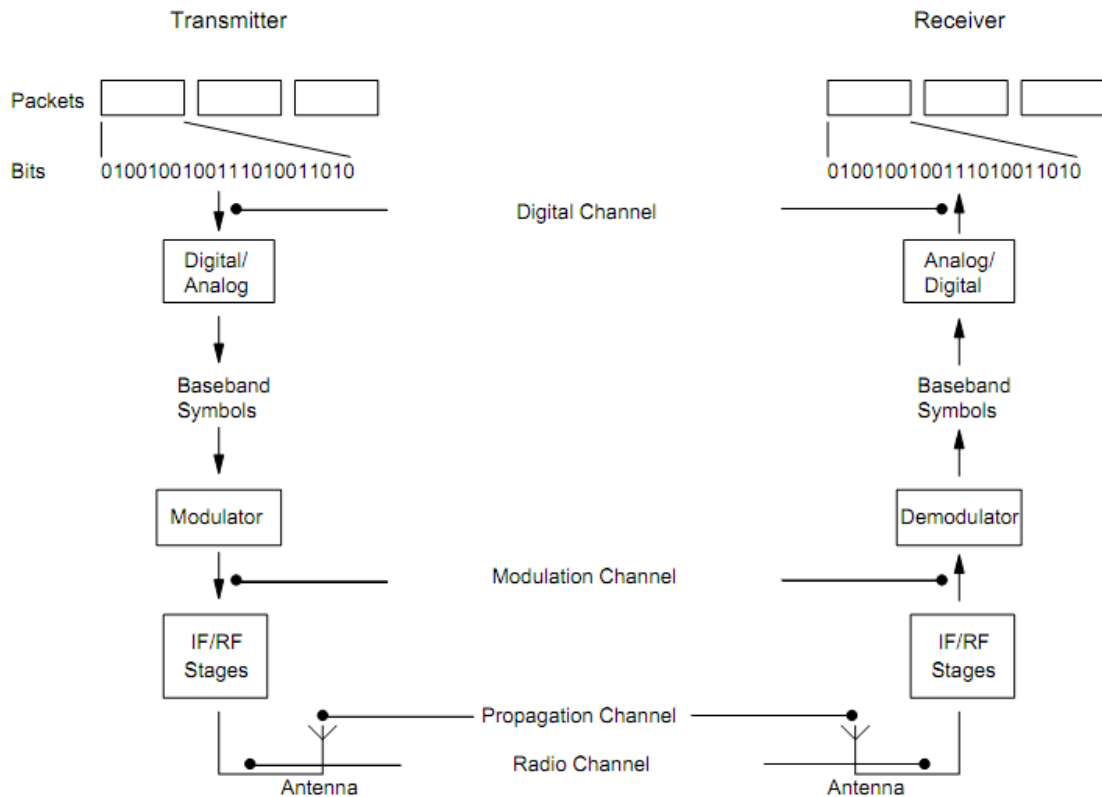


Fig 1 Channel Classification: Propagation, Radio, Modulation and Digital Channel

Path loss, shadowing and fading are three distinguished prime factors to influence the received signal on radio channel. Path loss is a deterministic effect and cause weakening of signal strength depending only on the distance between the transmitter and the receiver. Shadowing fluctuates the received signal strength at points with the same distance to the transmitter. It varies on the same time scale as the path loss does and not deterministic in nature. Fading cause significant attenuation changes in received signal strength within smaller time scales such as milliseconds or even microseconds. It is mostly present in multipath propagation environment, and random in nature. Above all three attenuating effects are mathematically combined to get the actual experienced attenuation of the radio channel as:

$$a(t) = a_{PL}(t) \cdot a_{SH}(t) \cdot a_{FA}(t)$$

2.1 Path loss

Path loss phenomena describe the power lessening of transmitted signal on mathematical expression depending on the distance travelled and frequency used. Under the assumption of stable environmental factor and the static transmitter and receiver, the received power on wireless channel decrease inversely proportional to square of distance between the transmitter and receiver. To calculate path loss model we made antennas consideration as passive and reciprocal. Two major characteristic of antennas are gain of antenna and radiation pattern, antenna gain signifies the signal amplification factor, and radiation pattern shows reference antenna gain compare with maximum antenna gain. To calculate the path loss only directional antenna are considered and antenna gain is written as

$$g = G_{\max} [\text{dB}] - G_{\text{att}}^{[\text{Tx Rx}]} [\text{dB}]$$

where G_{\max} is the antenna gain and

$G_{\text{att}}^{[\text{Tx Rx}]}$ is the value from the radiation pattern in LOS

Signal attenuation due to path loss in LOS over can be exactly calculated using the Maxwell equations. The ratio of received power (P_0) to transmitted power (P_t) is inversely proportional to the square of the distance and the square of the frequency used. Since the electromagnetic energy can't destroyed by free space it will same wherever it travels but energy per unit surface must decrease.

$$\frac{P_0}{P_t} = \left(\frac{\lambda}{4\pi d} \right)^2 g_{Tx} g_{Rx}$$

In realistic environment two ray model and empirical models are more popular. Two rays model calculate the received signal power by considering the direct wave and reflected wave. Empirical model give more precise estimation in urban, suburban and indoor environments. The Okumura-Hata model is based on extensive measurement campaigns made by Okumura in Japan and on a formula developed by Hata which

approximates the measured statistics for specified values [20]. For adaptive new environment the Lee Model is more suitable to model wireless channel. This model is also sub categorized in to area-to- area model and point-to-point model.

2.2 Fading

Interference due to scattered signals arriving at an antenna is called fading. It is responsible for the most rapid and violent changes of the signal strength itself as well as its phase. These signal variations are experienced on a small time scale, mostly a fraction of a second or shorter, depending on the velocity of the receiver [13]. The basis of origination fading in wireless communication is by the reception of multiple copies of the transmitted signal, each having followed a different path. Likewise multipath propagation, signal strength attenuation is also different in MIMO, since the signal paths have to pass different obstacles like windows, building walls of different materials, trees of different sizes and so on. Any kind of movement is encountered in the propagation environment makes channel time variant then the receiver also experiences variable signal strength due to mobility. In this way, the received signal fades due to interference.

The fading may vary with time, geographical position, radio frequency, etc. It is often modeled as a random process. Shifted and delayed waves might interfere destructively and therefore cause severe attenuation. In real scenario wireless transmission in ascertain environment including a certain velocity of objects is described by two values, the Doppler spread Δf_d and the delay spread $\Delta \tau$. Both parameter introduce from multipath reception, where each path may be characterized by a different Doppler shift and time delay. Doppler spread is caused by the motion of objects within the environment (which might be the transmitter, the receiver or scatterers), the delay spread is caused by the topology of the environment itself. Although the Doppler spread is a phenomenon in frequency, the overall result on the received signal is a time

selective behavior. For the delay spread; it is exactly the opposite with Doppler spread; is a phenomenon in time, the resulting impact on the received signal is a frequency selective behavior [14].

Mathematically, fading is usually modeled as a time-varying random change in the amplitude and phase of the transmitted signal. The terms fast and slow fading refer to the rate at which the magnitude and phase change imposed by the channel on the signal changes [20]. The coherence time is a measure of the minimum time required for the magnitude change of the channel to become uncorrelated from its previous value. Fast fading occurs when the coherence time of the channel is small relative to the delay constraint of the channel. In this situation, the amplitude and phase change imposed by the channel varies considerably over the period of use. Transmitter may take advantage of the variations in the channel conditions using time diversity to help increase robustness of the communication to a temporary deep fade in a fast-fading channel. Although a deep fade may temporarily erase some of the information transmitted, use of an error-correcting code coupled with successfully transmitted bits during other time instances (interleaving) can allow for the erased bits to be recovered. When the coherence time of the channel is large relative to the delay constraint of the channel this type of fading is called slow fading. In this duration, the amplitude and phase change imposed by the channel can be considered roughly constant. Slow fading can be caused by events such as shadowing, where a large obstruction such as a hill or large building obscures the main signal path between the transmitter and the receiver. Log-distance path loss model can simulate amplitude change caused by shadowing with log-normal distribution [20]. In a slow-fading channel, it is not possible to use time diversity because the transmitter sees only a single realization of the channel within its delay constraint. A deep fade therefore lasts the entire duration of transmission and cannot be mitigated using coding.

3 Multiple Input Multiple Output (MIMO)

3.1 Background

In a conceptually appealing, but somewhat simplistic manner, we may argue that the single transmitter and single receiver is exposed to fading, since the vector sum of the multiple propagation paths may add constructively. By contrast, in case of the multiple-input multiple-output (MIMO) scenario the chances are that at least one of the independently faded diversity-links benefits from the constructive interference of the received paths. Multiple antennas can be used at the transmitter and receiver, an arrangement called a MIMO system. It takes advantage of the spatial diversity that is obtained by spatially separated antennas in a dense multipath scattering environment. MIMO systems may be implemented in a number of different ways to obtain either a diversity gain to combat signal fading or to obtain a capacity gain. Generally, there are three categories of MIMO techniques. The first aims to improve the power efficiency by maximizing spatial diversity. Such techniques include delay diversity, space–time block codes (STBC) [7], [8] and space–time trellis codes (STTC) [9]. The second class uses a layered approach to increase capacity. One popular example of such a system is V-BLAST suggested by Foschini et al. [10] where full spatial diversity is usually not achieved. Finally, the third type exploits the knowledge of channel at the transmitter. It decomposes the channel coefficient matrix using singular value decomposition (SVD) and uses these decomposed unitary matrices as pre- and post-filters at the transmitter and the receiver to achieve near capacity [12].

3.2 MIMO Channel Capacity

In contrast with conventional single antenna system, the MIMO channel capacity can be increased m times where m is minimum no of antennas among transmit side or receive side without using additional transmit power or spectral bandwidth. MIMO

techniques can be broadly separated into two categories: spatial-multiplexing techniques and diversity techniques. Spatial-multiplexing technique simultaneously transmits the multiple independent data streams from multiple transmit antennas to achieve higher data speed [13]. I completely cover the spatial-multiplexing techniques in next preceding section. On the other hand, the diversity techniques are focused to receive the same information-bearing signals in the multiple antennas to improving the transmission reliability. A basic idea of the diversity techniques is to convert Rayleigh fading wireless channel into more stable AWGN-like channel without any catastrophic signal fading.

3.2.1 Spatial Multiplexing

Spatially multiplexed systems can transmit data at a higher speed and requires MIMO antenna configuration. In spatial multiplexing, a high rate signal is split into multiple lower rate streams and each stream is transmitted from a different transmit antenna in the same frequency channel. The receiver separates these streams into parallel channels if those signals arrive at receiver antenna with sufficient different spatial signatures. Spatial multiplexing can also be used for simultaneous transmission to multiple receivers, known as space-division multiple accesses. By scheduling receivers with different spatial signatures, good separability can be assured. This is a very powerful technique for increasing channel capacity at higher SNR. The maximum no of spatial streams is equal to lesser in the number of antennas at the transmitter or receiver side [13]. Spatial multiplexing can also be combined with precoding when the channel is known at the transmitter or combined with diversity coding when decoding reliability is in trade-off.

Consider the $N_R \times N_T$ MIMO system shown in Fig 2. Let H denote a channel matrix with the channel gain between the i_{th} transmit antenna and the j_{th} receive antenna, is writtiena as H_{ij} . where $i= 1, 2, 3, \dots, N_T$ and $j = 1, 2, 3, \dots, N_R$.

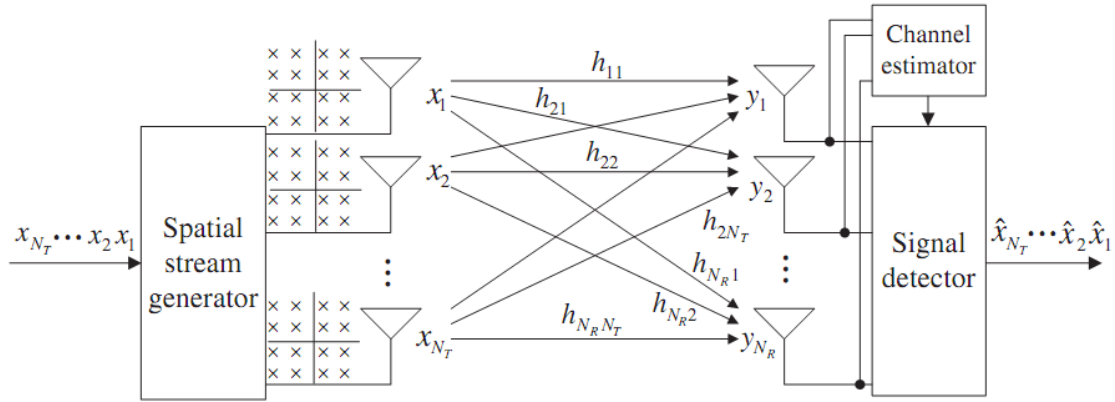


Fig 2 Spatially multiplexed MIMO systems

The spatially multiplexed user data is representing as $x = [x_1, x_2, x_3, \dots, x_{N_T}]$ and the corresponding received signals are represented as $y = [y_1, y_2, y_3, \dots, y_{N_R}]$. Here x_i and y_j are transmitted signal from i^{th} transmit antenna and received signal from j^{th} receive antenna. In wireless channel the transmitted waveform gets corrupted by noise η , typically referred to as additive white Gaussian noise (AWGN). Additive means noise gets added to the received signal, White signifies the spectrum of the noise is flat for all frequencies and Gaussian means the values of the noise η follows the Gaussian probability distribution function,

$$p(x_i) = \frac{1}{\sqrt{2\pi\sigma^2}} e^{-\frac{(x_i - \mu)^2}{2\sigma^2}} \quad \text{with mean } (\mu) = 0 \text{ and variance } (\sigma^2) = N_0/2$$

Now, the MIMO system is represented as

$$y = Hx + z$$

$$Y = h_1x_1 + h_2x_2 + h_3x_3 + \dots + h_{N_T}x_{N_T} + z \quad \text{where } z = [z_1, z_2, z_3, \dots, z_{N_R}]^T$$

There are many more techniques to detect the symbol in spatially multiplexed MIMO systems.

3.2.2 Diversity Coding

In diversity coding, a single stream is transmitted, but the signal is coded using techniques called space-time coding [8]. It is used when there is no channel

knowledge at the transmitter. Diversity coding exploits the independent fading in the multiple antenna links to enhance signal diversity. The signal is emitted from each of the transmit antennas with full or near orthogonal coding. Diversity techniques are used to extenuate degradation in the error performance due to unstable wireless channel subject to the multipath fading. In this section I study the basic concepts of antenna diversity techniques for AWGN channel, the slope of BER versus SNR curve is also simulated. The fundamental goal of the antenna diversity techniques is to convert an unstable time-varying wireless fading channel into a stable AWGN-like channel without significant instantaneous fading, thereby steepening the BER versus SNR curve.

3.2.3 Precoding

Precoding is multi-stream beam forming, in the precise definition. In more common words, it is conceived to be all spatial processing that occurs at the transmitter. In beam forming, the same signal is transmitted from each of the transmit antennas with appropriate phase weighting such that the signal power is maximized at the receiver input [19]. The advantages of precoding are to enhance the received signal strength, by making signals sent from different antennas add up constructively, and to reduce the multipath fading effect. In non-scattering situation, beam forming results in a well defined directional pattern, but in typical cellular conventional beams are not a good analogy. When the receiver has multiple antennas, the transmit beam forming cannot simultaneously maximize the signal level at all of the receive antennas, and precoding with multiple streams is used. Note that precoding necessitates knowledge of CSI at the transmitter.

4 Orthogonal Frequency Division Multiplexing (OFDM)

4.1 Introduction

Day by day, there has been increasing demands for wireless broadband communication systems within both the public and private sectors. Wireless channels are more contaminated than wired data channels and we can't preserve high QoS in wired channel so wired networks can't sustain extension to wireless data networks. The mobile wireless channel contains both a direct line-of-sight (LOS) radio wave and a large number of reflected radio waves that arrive at the receiver at different times. Those reflected, delayed waves interfere with the LOS wave and causes inter symbol interference (ISI) and it causes substantial degradation of network performance. Adaptive equalization may be one solution but due to high data rate and cost of system cause practical difficulties [3]. OFDM transmission system surmounts these problems with reducing the influence of multipath fading and makes complex equalizers unnecessary.

OFDM is a particular example of multicarrier transmission, where a single data stream is transmitted over a number of lower-rate subcarriers (SCs). One of the main reasons to use OFDM is to raise robustness against frequency-selective fading or narrowband interference [4]. In a single-carrier system, a single fade or interferer can cause the total information to loss, but in a multicarrier system, only a small percentage of the SCs will be affected. In this case error-correction coding can then be used to adjust for the few erroneous SCs.

In a classical parallel-data system, the total signal frequency band is divided into multiple non overlapping frequency sub channels. Each sub channel is modulated with a separate symbol, and then these sub channels are frequency multiplexed to avoid spectral overlap of channels to eliminate inter channel interference. Nevertheless, this

leads to inefficient use of the available spectrum. To grapple with this inefficiency, the ideas proposed in the mid-1960s were to use parallel data stream and FDM with overlapping sub channels, in which each, carrying a signaling rate, is spaced equal band apart in frequency to avoid the use of high-speed equalization and to combat impulsive noise and multipath distortion, as well as to use the available bandwidth totally [6]. The bandwidth consumption by conventional non overlapping multicarrier technique (FDMA) and OFDM are shown in Fig 3 below.

The term “orthogonal” signifies that there is a precise mathematical relationship between the frequencies of the carriers in the system. Normal FDM system lowers the spectrum efficiency by introducing guard bands between many carriers in the frequency domain and signals are received by using conventional filters and demodulators.

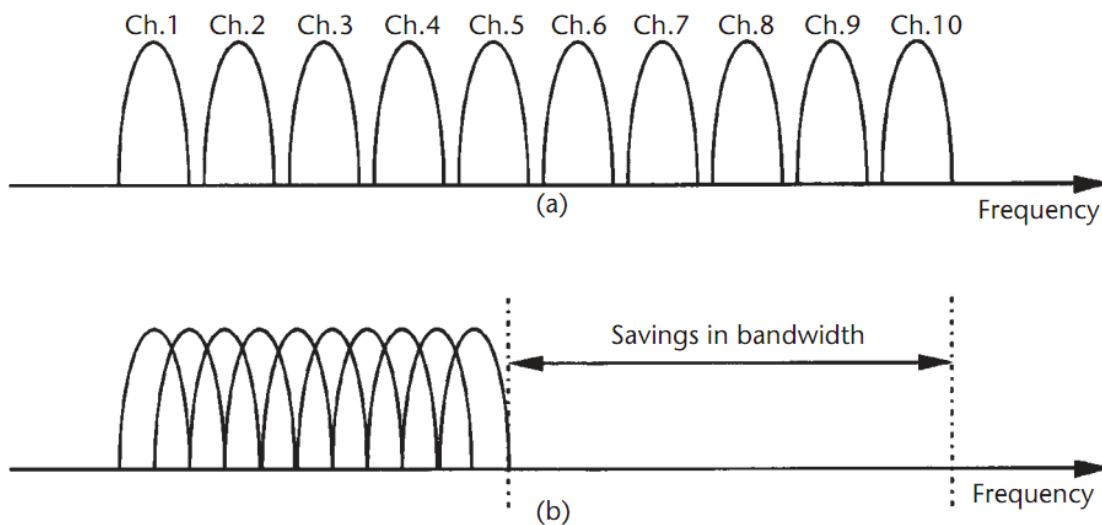


Fig 3 Concept of the OFDM signal: (a) conventional multicarrier technique, and (b) orthogonal multicarrier modulation technique

In 1971, Weinstein and Ebert applied the discrete Fourier transform (DFT) to parallel-data-transmission systems as part of the modulation and demodulation process [6]. The spectrum of the individual data of the sub channel is shown in Fig 4(a) Where the OFDM signal, multiplexed in the individual spectra with a frequency spacing equal to

the transmission speed of each sub carrier. There is no cross talk from other channels at the center frequency is shown in Fig 4(b). Therefore, by using DFT at the receiver and calculate correlation values with the center of frequency of each SC it is possible to recover the transmitted data with no cross talk. In addition, using the DFT-based multicarrier technique, FDM is achieved not by bandpass filtering but by baseband processing.

Moreover, to reject the banks of SC oscillators and coherent demodulators required by FDM, completely digital implementations could be built around special-purpose hardware performing the fast Fourier transform (FFT), which is an efficient implementation of the DFT. Powerful digital signal processor make high-speed, large size FFT chips commercially affordable in reasonable price. Using this device on both transmitter and receiver side we can implement efficient FFT techniques that reduce the number of operations from N^2 in DFT to $N \log N$ [12].

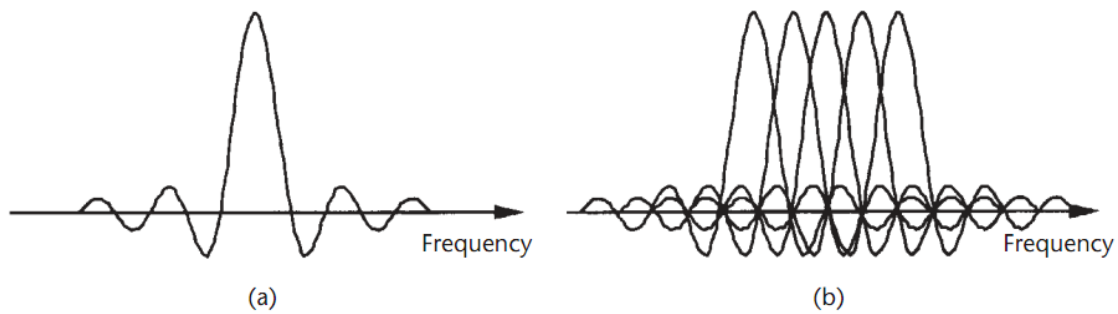


Fig 4 Spectra of (a) an OFDM sub channel, and (b) an OFDM signal

Despite the large peak-to-average-power ratio and more sensitive to frequency offset and phase noise drawbacks in OFDM there are great extent of advantages than single carrier system. The main merit of OFDM is the fact that the radio channel is divided into many narrowband, low-rate, frequency-nonselctive sub channels or subcarriers, so that multiple symbols can be transmitted in parallel, while maintaining a high spectral efficiency [5]. Furthermore OFDM is an efficient way to deal with multipath; for a given delay spread, the implementation complexity is significantly lower than

that of a single-carrier system with an equalizer. In relatively slow time-varying channels, it is possible to enhance capacity significantly by adapting the data rate per SC according to the SNR of that particular SC. OFDM is robust against narrowband interference because such interference affects only a small percentage of the SCs. OFDM makes single-frequency networks possible, which is especially attractive for broadcasting applications [12].

Current wireless data services are more often non-symmetrical. In Asymmetric digital subscriber line (ADSL) , 802.11 & 802.16 cases downlink channels contains more traffic than uplink channels. Different number of sub channels provides different data rates so these subcarriers provide physical layer supports non- symmetric data transmission.

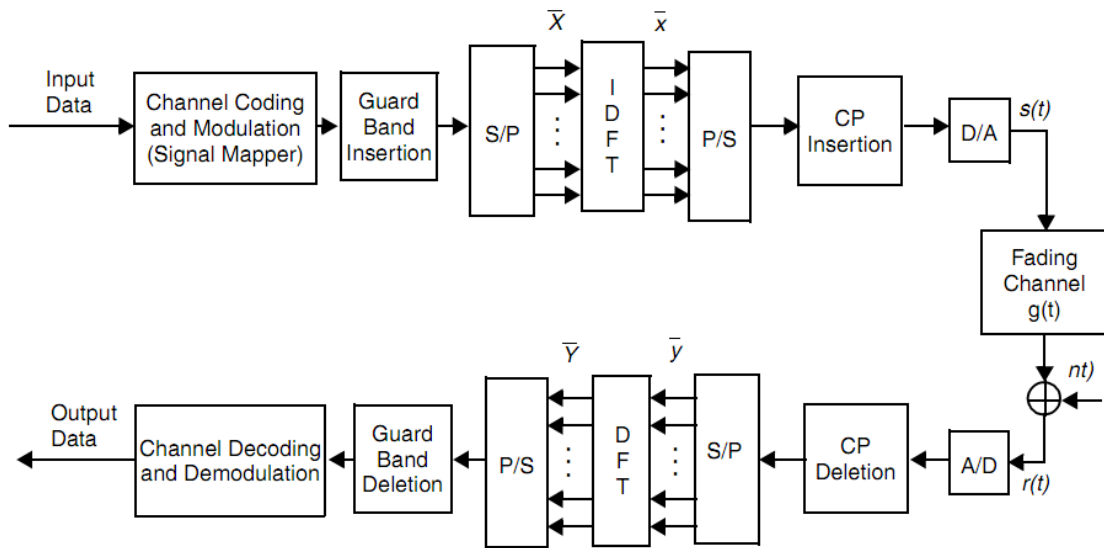


Fig 5 A Digital Implementation of a Baseband OFDM System

As shown in above Fig 5, OFDM is a block modulation scheme where a block of information symbols is transmitted in parallel on subcarriers. The time duration of an OFDM symbol is N times larger than that of a single-carrier system. An OFDM modulator can be implemented as an inverse discrete Fourier transform (IDFT) on a block of information symbols followed by an analog-to-digital converter (ADC). To

mitigate the effects of inter symbol interference (ISI) caused by channel time spread, each block of IDFT coefficients is typically preceded by a cyclic prefix (CP) or a guard interval consisting of samples, such that the length of the CP is at least equal to the channel length. Under this condition, a linear convolution of the transmitted sequence and the channel is converted to a circular convolution. As a result, the effects of the ISI are easily and completely eliminated. Moreover, the approach enables the receiver to use fast signal processing transforms such as a fast Fourier transform (FFT) for OFDM implementation.

4.2 Cyclic Prefix

The OFDM guard interval can be inserted in two different ways. Multiband OFDM in ultra wide band (UWB) communication use the approach of zero padding (ZP) that pads the guard interval with zeros. The other is the cyclic extension of the OFDM symbol with CP (cyclic prefix) or CS (cyclic suffix). CP is to extend the OFDM symbol by copying the last samples of the OFDM symbol into its front. Let denote the length of CP in terms of samples. Then, the extended OFDM symbols now have the duration of $T_{sym} = T_{sub} + T_G$. Fig 6 shows two consecutive OFDM symbols, each of which has the CP of length , while illustrating the OFDM symbol of length .

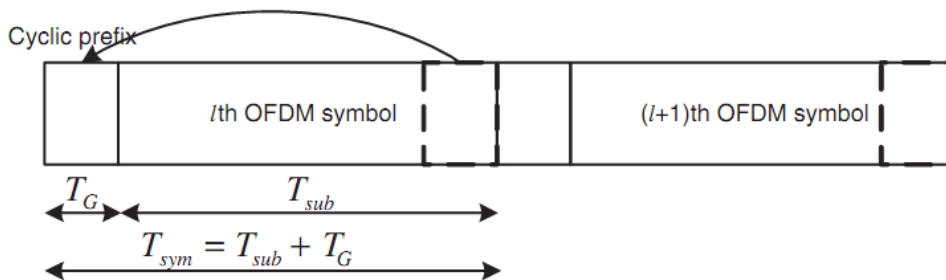


Fig 6 OFDM symbols with CP

It can be seen from above figure that if the length of the guard interval (CP) is set longer than or equal to the maximum delay of a multipath channel, the ISI effect of an OFDM symbol (plotted in a dotted line) on the next symbol is limited within the guard

interval so that it may not impress the FFT of the next OFDM symbol, taken for the duration of T_{sub} . This implies that the guard interval longer than the maximum delay of the multipath channel asserting the orthogonality among the subcarriers. As the continuity of each delayed subcarrier has been justified by the CP, its orthogonality with all other subcarriers is maintained over.

Channel delay spread causes ISI which cause irreducible error floor, hence limiting maximum data rate. However, symbol duration of each subcarrier in OFDM is N times longer than that of single carrier system. Therefore, OFDM is more robust to delay spread than single carrier. Although OFDM suffers less ISI than single carrier, it still experiences some ISI. This ISI can be totally avoided by using cyclic prefix whose length is equal to or longer than maximum channel delay spread [13]. Due to cyclic prefix, linear convolution of the channel impulse response and the signal becomes cyclic convolution.

4.3 The Peak to Average Power Ratio

An OFDM signal comprises of a number of independently modulated SCs. The transmit signals in an OFDM system can have high peak values in the time domain since many subcarrier components are added via an IFFT operation, which can give a large peak-to-average power ratio (PAPR) when added up coherently. When M signals are added with the same phase, they produce a peak power that is M times the average power.

The peak power is defined as the power of a sine wave with amplitude equal to the maximum envelope value. Hence, an unmodulated carrier has a PAPR of 0 dB. An alternative measure of the envelope variation of a signal is the Crest factor, which is defined as the maximum signal value divided by the RMS signal value. For an unmodulated carrier, the Crest factor is 3 dB. This 3-dB difference between the PAPR

and crest factor also holds for other signals, provided that the center frequency is large in comparison with the signal bandwidth [12]. The complex data block for the OFDM signal to be transmitted is given by

$$x(t) = \frac{1}{\sqrt{N}} \sum_{n=0}^{N-1} X_n \cdot e^{j2\pi n \Delta f t} \quad 0 \leq t \leq NT$$

And the ratio between the maximum power and the average power of the complex passband signal $x(t)$ is written as

$$PAPR\{x(t)\} = \frac{\max | \operatorname{Re} x(t) | e^{j2\pi f_c t} |^2}{E \{ | \operatorname{Re} x(t) e^{j2\pi f_c t} |^2 \}}$$

4.4 PAPR Determining Elements

The PAPR in particular communication system depends on different factors. Some of prime factor are No of subcarriers, over sampling rate, modulation schemes etc.

4.4.1 Number of sub-carriers

In multicarrier system the noise floor arises proportional to subcarrier number which results PAPR increment. Different number of subcarrier forms different PAPR performance. According to the graph plotted in QPSK modulation with different number of subcarrier in same environment in Fig 7. The PAPR exceeds 10 dB accounts for only 0.1% of transmitted signal approximately when the subcarrier number is 64, but when the subcarrier number increased to 256, the PAPR surpasses 10 dB accounts for almost 1% of transmitted OFDM signals. From this justification it can be said that subcarrier number is very vital factor to determine PAPR.

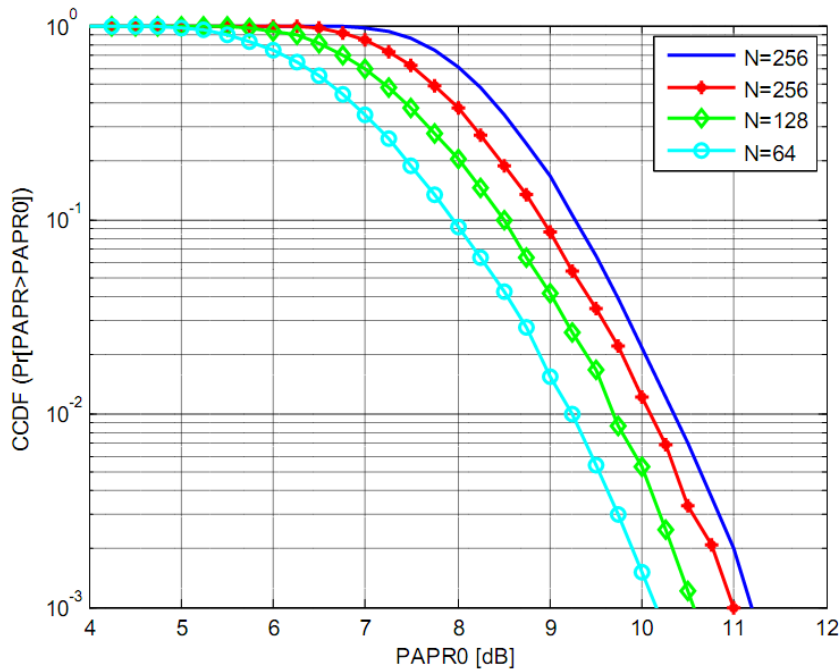


Fig 7 PAPR performance with different values of subcarriers

4.4.2 Oversampling rate

In real implementation, it is difficult to describe continuous-time OFDM signal in finite digital system so the sampling is tradeoff between QoS and system capacity. The prime motive of oversampling is to avoid missing of peak signal. Over-sampling plays an important role for reflecting the variation characteristics of OFDM symbols in time domain. Fig 8 shows the plot of different over-sampling rate with fixed probability. To cope with PAPR problem product of no of subcarrier (N) and oversampling rate (L) point IFFT/FFT of original data with $(L-1) \times N$ zero padding operation. Based on the plot it can be said that oversampling factor $L=4$ is sufficient to catch the peak.

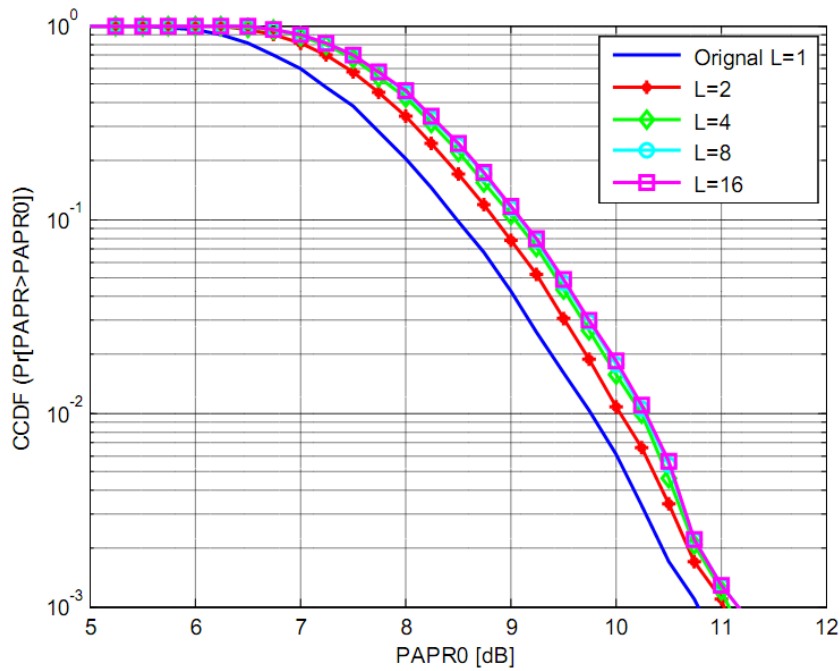


Fig 8 PAPR performance with different values of oversampling rate

4.4.3 Modulation Schemes

Various modulation scheme can be implemented in multicarrier system and based on their characteristics they show different PAPR performance rating. Fig 9 show small variation in PAPR performance due to modulation type, moreover higher order modulation are more pathetic PAPR performance but minimum influence in overall performance.

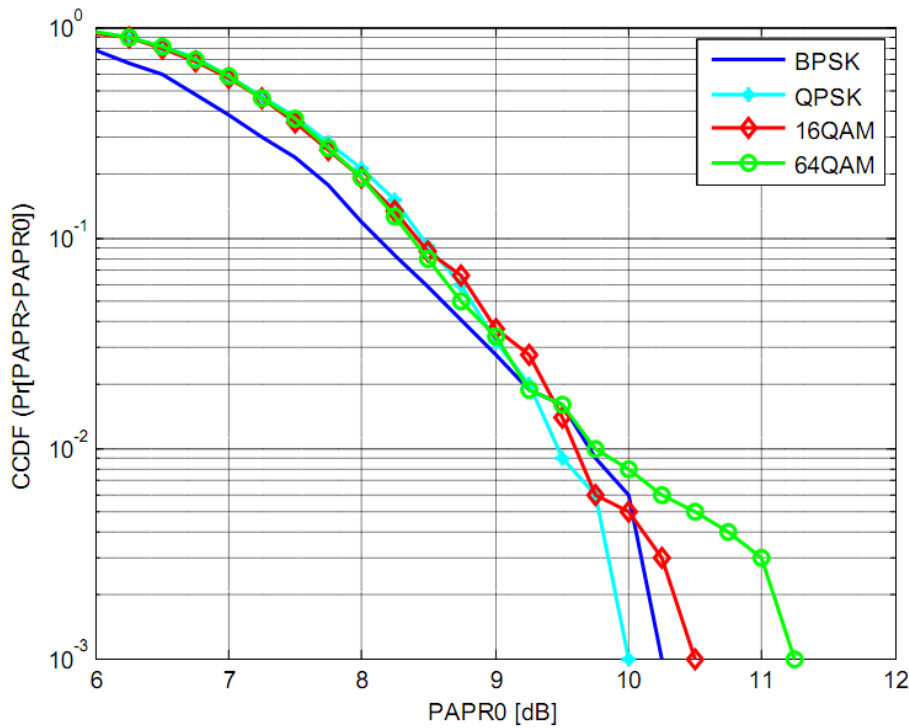


Fig 9 PAPR performance with various modulation schemes

4.5 PAPR Reduction Technique

A large PAP ratio brings disadvantages like an increased complexity of the analog-to-digital (A/D) and digital-to-analog (D/A) converters and a reduced efficiency of the RF power amplifier. There is nonlinearity between input and output characteristics of power amplifier and described in terms of Input Back-Off (IBO) and Output Back-Off (OBO)

$$IBO = 10 \text{ Log } 10 \frac{P_{in \max}}{P_{in}} \quad OBO = 10 \text{ Log } 10 \frac{P_{out \max}}{P_{out}}$$

The Cumulative Distribution Function (CDF) is major parameters to measure the efficiency of any PAPR technique. Normally, the Complementary CDF (CCDF) is

used instead of CDF, which helps us to measure the probability that the PAPR of a certain data block exceeds the given threshold.

Implementing the Central Limit Theorem for multi-carrier signal with a large number of sub-carriers follows a Gaussian distribution with mean zero and a variance of 0.5. So Rayleigh distribution is followed for the amplitude of the multi-carrier signal, whereas a central chi-square distribution with two degrees of freedom is followed for the power distribution of the system.

The CDF of the amplitude of a signal sample is given by $F(z) = 1 - \exp(-z)$

The CCDF of the PAPR of the data block is desired in this thesis to compare outputs performance of various PAPR reduction techniques. This is given by

$$\begin{aligned} P(\text{PAPR} > z) &= 1 - P(\text{PAPR} \leq z) \\ &= 1 - F(z)^N \\ &= 1 - (1 - \exp(-z))^N \end{aligned}$$

To reduce the PAPR, several techniques have been proposed; basically they are divided in five categories. First one is signal distortion techniques, which reduce the peak amplitudes simply by nonlinearly distorting the OFDM signal at or around the peaks. This can be achieved by clipping, peak windowing, and peak cancellation. Second one is coding techniques that use a special forward error correction (FEC) code set that excludes OFDM symbols with a large PAPR. Third one scrambling technique, which scrambles each OFDM symbol with different scrambling sequences and select the sequence that gives the smallest PAPR value. The next one is adaptive predistortion technique, which can compensate the nonlinear effect of a high power amplifier (HPA) in OFDM systems [21]. It can address the time variations of nonlinear HPA by automatically modifying the input constellation with minimum RAM and memory lookup encoder. The last one method is DFT-spreading where the input signal is spreaded with DFT and subsequently taken into IFFT. This is known as

the Single Carrier-FDMA (SC-FDMA), and it can reduce the PAPR of OFDM signal to the level of single-carrier transmission.

Normally, the performance of PAPR reduction techniques can be evaluated in the following three aspects:

- In-band ripple and out-of-band radiation that can be observed via the power spectral density(PSD)
- Dispersion of the crest factor or PAPR, which is given by the corresponding CCDF
- Coded and uncoded BER performance.

4.5.1 Signal distortion techniques (clipping, peak windowing, peak cancellation)

Clipping

Clipping method limits the amplitude of signal to some desired maximum level by curtail the signal. Although clipping is definitely the simplest solution, there are a few problems associated with it. First, by distorting the OFDM signal amplitude, a kind of self-interference is introduced that degrades the BER. Second, the nonlinear distortion of the OFDM signal significantly increases the level of the out-of-band radiation. The second effect can be understood easily by viewing the clipping operation as a multiplication of the OFDM signal by a rectangular window function that equals one if the OFDM amplitude is below a threshold and less than one if the amplitude needs to be clipped. The spectrum of the clipped OFDM signal is found as the input OFDM spectrum convolved with the spectrum of the window function. The out-of-band spectral properties are mainly determined by the wider spectrum of the two, which is the spectrum of the rectangular window function. This spectrum has a very slow roll off that is inversely proportional to the frequency.

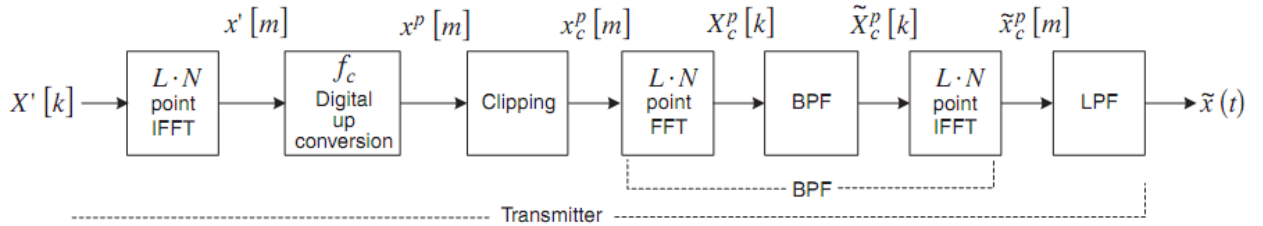


Fig 10 Block diagram of a PAPR reduction scheme using clipping and filtering

Block diagram of clipping and filtering technique for PAPR reduction is shown in Fig 10; where L is the oversampling factor and N is the number of subcarriers. In this scheme, the L-times oversampled discrete-time signal $x'[m]$ is generated from the IFFT. Let denote the clipped version of $x^p[m]$ which is expressed as

$$x_c^p [m] = \begin{cases} x^p [m] & \text{if } |x^p [m]| < A \\ \frac{x^p [m]}{|x^p [m]|} \cdot A & \text{otherwise} \end{cases}$$

Where A is the threshold clipping level and clipping ratio (CR) is defined as the clipping level normalized by the RMS values σ of OFDM signal, such that $CR = A / \sigma$. It has been known that σ is square root of no of subcarriers for baseband OFDM signal and square root of no of half subcarriers for passband OFDM signals, respectively.

Peak windowing

Out-of-band problem of clipping technique is amending by a new approach of multiplying large signal peaks with a certain nonrectangular window with good spectral properties. To minimize the out-of-band interference, ideally the window should be as narrowband as possible then again, the window should not be too long in the time domain because that implies that many signal samples are affected, which increases the BER. Examples of suitable window functions are the cosine, Kaiser, and hamming windows.

Peak cancellation

The fundamental guideline of all distortion techniques is to reduce the amplitude of samples whose power exceeds a certain threshold. In the case of clipping and peak windowing, this was done by a nonlinear distortion of the OFDM signal, which resulted in a certain amount of out-of-band radiation. This undesirable effect can be prevented by performing a linear peak-cancellation technique, whereby a time-shifted and scaled-reference function is subtracted from the signal, such that each subtracted reference function reduces the peak power of at least one signal sample. By selecting an appropriate reference function with approximately the same bandwidth as the transmitted signal, it can be assured that the peak power reduction will not cause any out-of-band interference.

One example of a suitable reference signal is a sinc function. A limitation of a sinc function is that it has infinite support. Hence, for practical use, it has to be time limited in some way. The appropriate solution for this unnecessary out-of-band interference is to multiply it by a windowing function. Raised cosine window can be used in this situation. If the windowing function is the same as that used for the windowing of the OFDM symbols, then it is assured that the reference function has the same bandwidth as the regular OFDM signals. Hence, peak cancellation will not degrade the out-of-band spectrum properties. By making the reference signal window narrower, a trade-off can be made between less complexity in the peak-cancellation calculations and some increase in the out-of-band power.

4.5.2 Coding techniques

A Limitation of distortion techniques is that symbols with a large PAP ratio suffer more degradation, so they are more vulnerable to errors. Forward error correcting (FEC) code can be applied across several OFDM symbols to minimize degradation of symbol with large PAPR. By doing so, errors caused by symbols with a large degradation can be corrected by the surrounding symbols. In a Coded OFDM system,

the error probability is no longer dependent on the power of individual symbols, but rather on the power of a number of consecutive symbols.

Since such a low symbol-error probability technique may be good enough for real time circuit switched traffic, suchlike voice, it may still cause problems for packet data. A packet with too many large PAP ratio symbols will have a large probability of error. Such packets occur only very infrequently, as shown above, but when they occur, they may never come through because every retransmission of the packet has the same large error probability.

4.5.3 Symbol scrambling

The emersion of high power signal in OFDM system is due to the superposition (IFFT operation) of multiple subcarrier signals. Among the multiple sequences the best one sequence with lowest PAPR is selected.

In symbol scrambling each OFDM symbol is multiplied by scrambling sequences, among the result of scrambled symbols with the smallest PAPR is transmitted from modulator. Symbol scrambling does not, however, try to combine FEC and PAPR reduction such as is done by the complementary codes. Scrambling techniques were first proposed under the names partial transmit sequences and selected mapping. The difference between the two is that the first applies scrambling rotations to groups of SCs, while the latter only applies independent scrambling rotations to all SCs. For uncorrelated scrambling sequences, the resulting OFDM signals and corresponding PAP ratios will be uncorrelated, so if the PAPR for one OFDM symbol has a probability p of exceeding a certain level without scrambling, the probability is decreased to p^k by using k scrambling codes. Hence, Symbol scrambling does not guarantee a PAPR below some low level; rather, it decreases the probability that high PAPR will occur.

4.5.3.1 Selected Mapping

In selective mapping (SLM) technique the actual transmit signal lowest PAPR is selected from a set of sufficiently different signals which all represents the same information. SLM Technique is very flexible as they do not impose any restriction on modulation applied in the subcarriers or on their number. Block diagram of SLM Technique is shown in Fig 11.

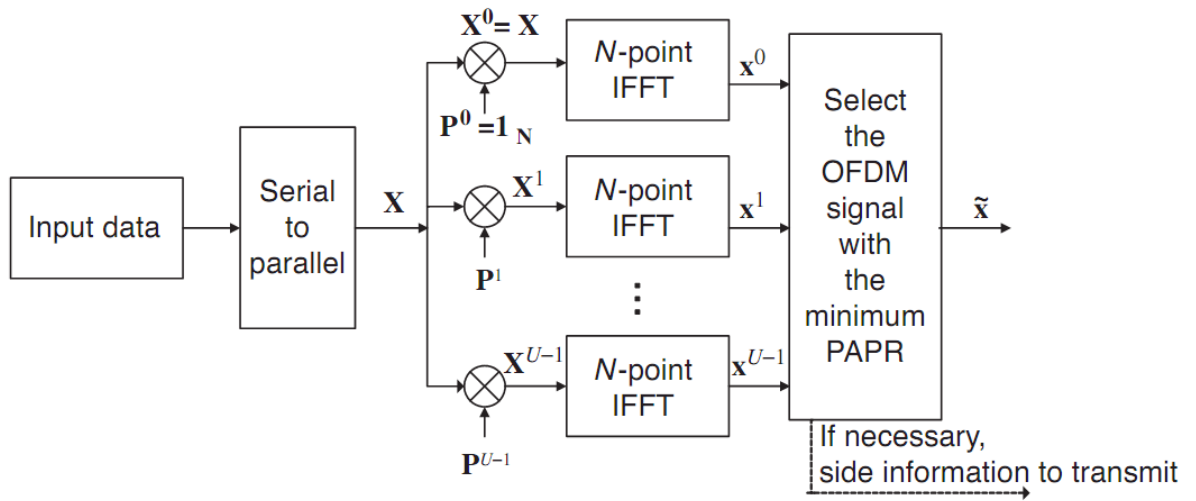


Fig 11 Block diagram of selective mapping (SLM) technique for PAPR reduction

The CCDF of the original signal sequence's PAPR above a threshold $PAPR_0$ is written as $\Pr\{PAPR > PAPR_0\}$. Thus CCDF can be rewritten as $[\Pr\{PAPR > PAPR_0\}]^K$ for K statistical autonomous signal waveforms, and the probability of PAPR larger than a threshold value can be written as

$$P\{PAPR_{low} > PAPR_0\} = (P\{PAPR > Z\})^M = ((1 - \exp(-z))^N)^M$$

Let's define data stream after serial to parallel conversion as $X = [X_0, X_1, \dots, X_{N-1}]^T$

Where $n = 0, 1, 2, \dots, N-1$

Then define the random sequence $P_m = [P_{m,0} P_{m,1} \dots P_{m,N-1}]^T$

Where $m=1,2,\dots,M$ and rotation factor $(P_{m,n}) = \text{Exp}(j\varphi_{n,m})$

The N different sub-carriers are modulated with these vectors respectively so as to generate candidate OFDM signals. This process can also be seen as performing dot product operation on a data block X_n with rotation factor P_m .

$$S_m = [X_0 P_{m,0} X_1 P_{m,1} \dots X_{N-1} P_{m,N-1}]^T \quad m=1,2,\dots,M$$

and then transfer these M OFDM frames from frequency domain to time domain by performing IFFT calculation. The entire process is given by

$$x_m(t) = \frac{1}{\sqrt{N}} \sum_{n=0}^{N-1} x_n P_{m,n} e^{j2\pi n \Delta f t} \quad 0 \leq t \leq NT$$

Where $\Delta f = 1/NT$, here NT is the duration of an OFDM data block.

Finally, the one which possess the smallest PAPR value is selected for transmission. Its mathematical expression is given as

$$x_d = \text{argmin}_{1 \leq m \leq M} (\text{PAPR}(x_m))$$

Where $\text{argmin}()$ represents the argument of minimum value

Receiver need to know which sequence is linked to the smallest PAPR among M different candidates, in order to correctly demodulate the received signal. Regarding the principles of SLM algorithm, it is well known that the ability of PAPR reduction using SLM is affected by the route number M and subcarrier number N .

4.5.3.2 Partial Transmit Sequence

The basic idea of partial transmit sequences (PTS) algorithm is to separate the original OFDM sequence into respective sub-sequences, and for each sub-sequence, multiplied

by different weights until an optimum value is chosen, which is a technique for improving the statistics of a multi-carrier signal. PTS algorithm was first proposed by Muller S H, Huber J B [23].

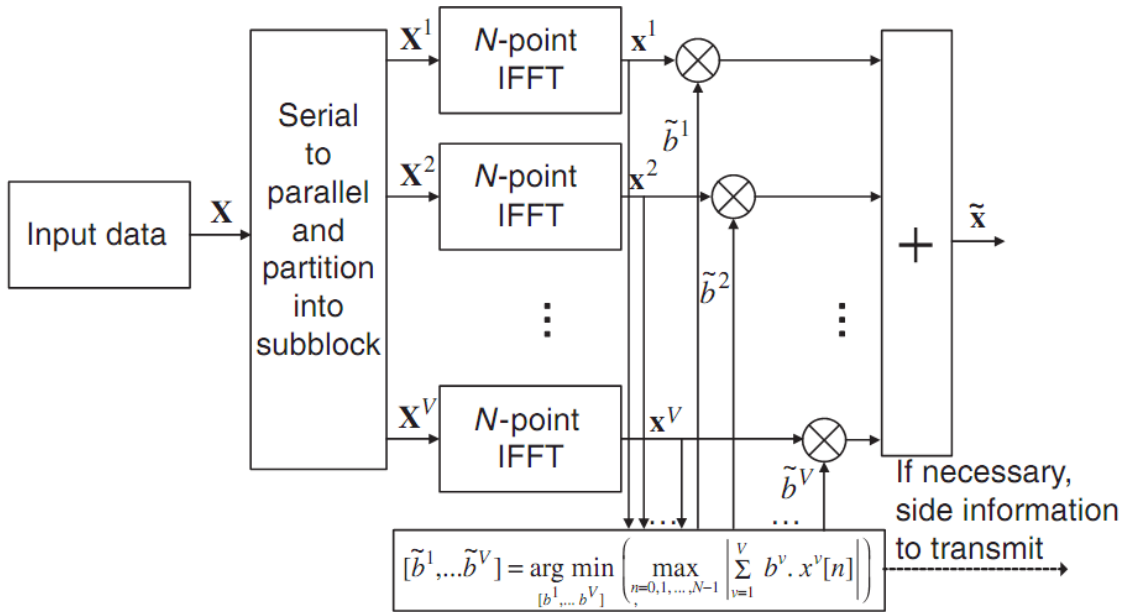


Fig 12 Block diagram of partial transmit sequence technique

The PTS method divides an input data block of N symbols into V disjoint subblocks as

$$\mathbf{X} = [\mathbf{X}^0, \mathbf{X}^1, \mathbf{X}^2, \dots, \mathbf{X}^{V-1}]^T$$

Where \mathbf{X}^i are the consecutively located subblocks that are also of equal size. Different from the SLM technique in which scrambling is applied to all subcarriers, scrambling (rotating its phase independently) is applied to each subblock in the PTS technique (Fig 12). Then each partitioned subblock is multiplied by a corresponding complex phase factor $b^v = e^{j\phi^v}$

Where $v = 1, 2, \dots, V$, subsequently taking its IFFT to yield

$$x = IFFT \left\{ \sum_{v=1}^V b^v X^v \right\} = \sum_{v=1}^V b^v \cdot IFFT\{X^v\} = \sum_{v=1}^V b^v x^v$$

Where $\{X^v\}$ is referred as a PTS

The phase vector is chosen so that the PAPR can be minimized as

$$[b^1, \dots, b^V] = \arg \min \left(\max \left| \sum_{v=1}^V b^v x^v[n] \right| \right)$$

Then, the corresponding time-domain signal with the lowest PAPR vector can be expressed as

$$\tilde{x} = \sum_{v=1}^V \tilde{b}^v x^v$$

In general, the selection of the phase factors is limited to a set of elements to reduce the search complexity. As the set of allowed phase factors is

$$b = e^{j2\pi i/w} \quad \text{where } i=0, 1, 2, \dots, w-1$$

sets of phase factors should be searched to find the optimum set of phase vectors. Therefore, the search complexity increases exponentially with the number of subblocks.

The PTS method needs V IFFT operations for each data block and $\lceil \log_2 W^V \rceil$ bits of side information. The PAPR performance of the PTS technique is majorly affected by the number of subblocks, the number of the allowed phase factors and the subblock partitioning [13]. In fact, there are three different kinds of the subblock partitioning schemes: adjacent, interleaved, and pseudo-random. Complexity of searching for the optimum set of phase vector increases with the higher the number of subblocks.

4.5.4 Adaptive Predistortion Technique

High power amplifier (HPA) efficiency is the main concerns in wireless communication systems because of it directly affect the size, power consumption, and cost. Simultaneously, HPA linearity is critical for linear modulation schemes. Adaptive predistortion technique compensates for the nonlinear distortion of an HPA by predistorting the input waveform. Predistortion is applied in the form of digital gain and phase changes that are functions of instantaneous input waveform amplitudes [22]. Convergence of the algorithm is measured on the basis of out-of-band emission levels. The use of adaptive predistortion technique not only improves the overall efficiency by allowing amplifier operation closer to the saturation point but also give cost-effective method to linearise the transmit power amplifiers of spectrally efficient communication in digital baseband system. From a signal processing point of view, the functional structure of the pre-distorter is mainly determined by the decision which model to choose, as well as by the selected adaptive algorithm.

4.5.5 DFT-spreading Technique

If DFT-spreading technique, use the same size IFFT is used as a spreading code, then, the OFDMA system becomes equivalent to the Single Carrier FDMA (SC-FDMA) system because the DFT and IDFT operations virtually compensate each other. For this reason, the transmit signal will have the same PAPR as in a single-carrier system. The equivalency is easily linked from the Fig 13. The effect of PAPR reduction depends on the way of assigning the subcarriers. There are two different approaches of assigning subcarriers among users: DFDMA (Distributed FDMA) and LFDMA (Localized FDMA). Here, DFDMA distributes M DFT outputs over the entire band (of total N subcarriers) with zeros filled in unused subcarriers, When DFDMA distributes DFT outputs with equi-distance $(S) = N/M$, it is referred to as

IFDMA(Interleaved FDMA) where S is called the bandwidth spreading factor, whereas LFDMA allocates DFT outputs to M consecutive subcarriers in N subcarriers.

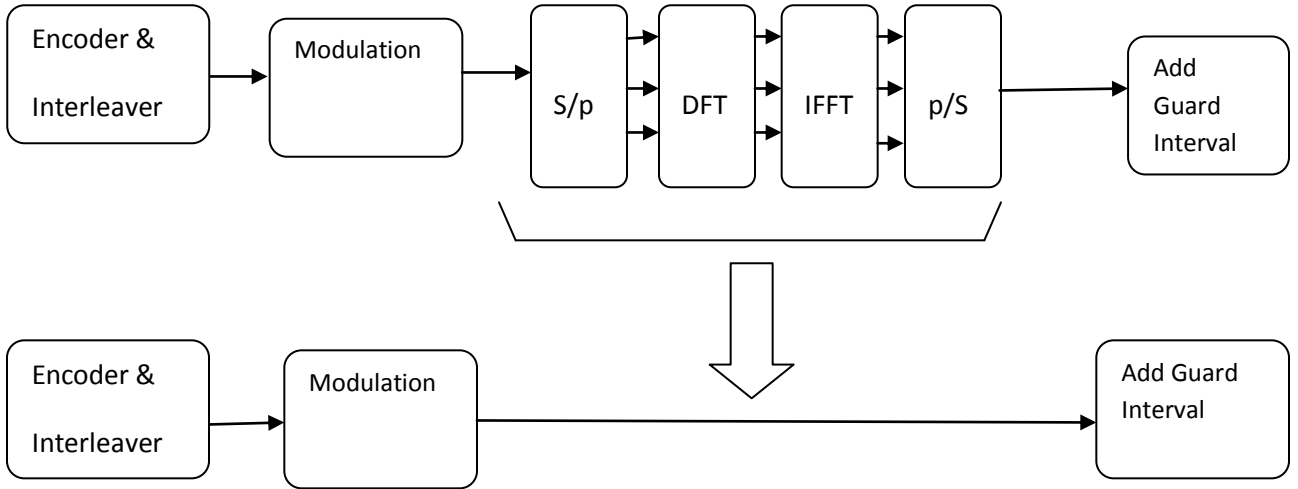


Fig 13 Equivalence of OFDMA system with DFT-spreading code to a single-carrier system

Fig 14 shows the subcarrier allocation of Interleaved FDMA, Distributed FDMA and Localized FDMA. Mathematically the Different s DFT-spreading can be written as

$$\hat{X}[k] = \begin{cases} X[S * k], & k = 0,1,2 \dots \dots, M - 1 \\ 0, & \textit{otherwise} \end{cases} \quad \text{IFDMA}$$

$$\hat{X}[k] = \begin{cases} X[\hat{S} * k], & k = 0,1,2 \dots \dots, M - 1 \\ 0, & \textit{otherwise} \end{cases} \quad \text{DFDMA}$$

$$\hat{X}[k] = \begin{cases} X[k], & k = 0,1,2 \dots \dots, M - 1 \\ 0, & k = M, M + 1, \dots \dots, N - 1 \end{cases} \quad \text{LFDMA}$$

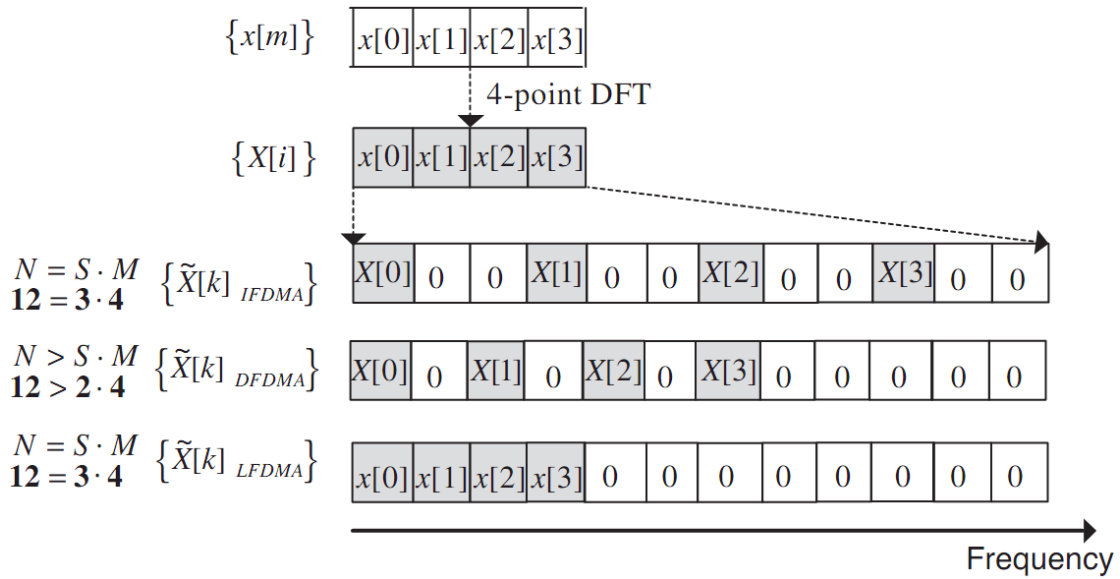


Fig 14 Examples of DFT spreading for IFDMA, DFDMA and LFDMA: three users with $N=12$; $M= 4$

Table 1 Comparison effects of PAPR reduction technique

Method	Distortion	Power increase	Data rate loss	Operation Done at Tx and Rx	
Clipping	yes	no	no	Tx: clipping Rx: none	
coding	no	no	yes	Tx: coding and table searching Rx: decoding and table searching	
Symbol Scrambling	SLM	no	no	yes	Tx: M times IDFT operations Rx: side information extraction, inverse SLM
	PTS	no	no	yes	Tx: V times IDFT operations Rx: side information extraction, inverse PTS
Adaptive predistortion	no	no	yes	Tx: peak reduction tone are overlapped with data tone Rx: receiver decodes only data tones	
DFT spreading	no	no	yes	Tx: D times IDFT operation, D-1 times interleaving Rx: side information extraction, de-interleaving	

5 Channel Estimation

5.1 Background

The radio channels in wireless communication system are usually multipath fading channels, the region of this cause received signal is usually distorted by the channel characteristics. By placing spatially separated multiple antenna elements at both ends of the transmission link, MIMO technologies can improve the link reliability and provide a significant increase of the link capacity [24]. In order to retrieve the transmitted bits, the channel effect must be estimated and compensated in the receiver. The location of channel estimation is figured out in Fig 15. In order to choose the channel estimation technique for the MIMO-OFDM system under consideration, many different aspects of implementations, including the required performance, computational complexity and time-variation of the channel must be taken into account.

The performance enhancement brought by MIMO systems mainly attributes to the space time techniques which aimed to remove the channel effects at both transmission and detection phase. Channel state information (CSI) generated by the channel estimator, is either fed back to the transmitter side to construct beamforming weight vector or sent into the detection block.

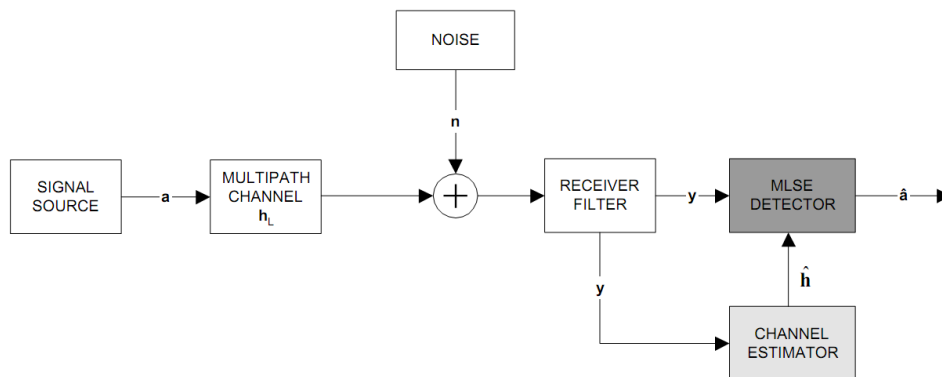


Fig 15 Block diagram of channel estimation

There are mainly four types of attributes to classify the channel estimator, which are pilot arrangement, estimation theory, processing domain and estimation iteration. According to pilot symbol arrangement the channel estimator are categorized into Block type, Comb type and Lattice type. Similarly in estimation theory, least square (LS) estimation and minimum mean square estimation (MMSE) are categorized. There are two domain which is time domain and frequency domain, so estimator can be constructed in both domains. Lastly the estimator can be separated based on no of iteration used to predict CSI, that are direct method and iterative method.

5.2 Pilot Structure

In general, the channel can be estimated by using a preamble or pilot symbols known to both transmitter and receiver, which employ various interpolation techniques to estimate the channel response of the subcarriers between pilot tones. In general, data signal as well as training signal, or both, can be used for channel estimation. Pilot structure is a signal usually in single frequency, transmitted over a communications channel for supervisory, control, equalization, continuity, synchronization, or reference purposes. Depending on the arrangement of pilots, three different types of pilot structures are considered: block type, comb type, and lattice type and functional block diagram of pilot based estimator is shown in Fig 16.

In block type pilot arrangement, OFDM symbols with pilots at all subcarriers are transmitted periodically for channel estimation and suitable for frequency-selective channels. Using these pilots, a time-domain interpolation is performed to estimate the channel along the time axis. Block-type pilot arrangement is suitable for frequency selective channels. To keep track of time-varying channel characteristics, the pilot symbols are limited within coherence time. As the coherence time is given in an inverse form of the Doppler frequency f_{Doppler} in the channel, the pilot symbol period must satisfy the following inequality:

$S_t \leq 1/ f_{\text{Doppler}}$ where S_t : is the period of pilot symbol,
 f_{Doppler} : is the Doppler spreading

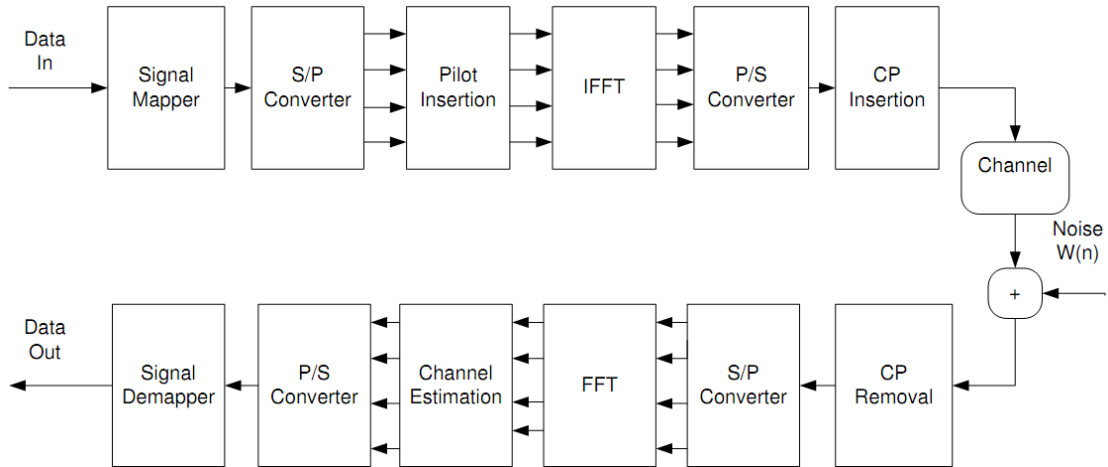


Fig 16 OFDM system with pilot based channel estimation

In Comb-type pilot arrangement, every OFDM symbol has pilot tones at the periodically-located subcarriers, which are used for a frequency domain interpolation to estimate the channel along the frequency axis. Comb type pilot arrangement is suitable for fast-fading channels. Pilot symbols are placed within coherent bandwidth to keep track of the frequency-selective channel characteristics. As the coherence bandwidth is determined by an inverse of the maximum delay spread σ_{max} , the pilot symbol period must satisfy the following inequality:

$S_f \leq 1/ \sigma_{\text{max}}$ where S_f : period of pilot tones in frequency
 σ_{max} : maximum delay spread

In Lattice-type pilot arrangement, pilot tones are inserted along both the time and frequency axes with given periods. The pilot tones scattered in both time and frequency axes facilitate time/frequency-domain interpolations for channel estimation. In order to keep track of the time-varying and frequency-selective channel

characteristics, the pilot symbol arrangement must satisfy both Block type and Comb type inequality.

$$S_t \leq 1/ f_{\text{Doppler}} \quad \& \quad S_f \leq 1/ \sigma_{\text{max}}$$

5.3 Training Symbol Based Channel Estimation

Training symbols based channel estimation usually providing a good performance. Overhead of training symbols like preamble symbol or pilot symbol reduce the transmission efficiencies. The least-square (LS) and minimum-mean-square-error (MMSE) techniques are widely used for channel estimation when training symbols are available [13]. The least-square channel estimation method estimate the channel based on the least value of errors square without using any knowledge of the statistics of the channels, the LS estimators are calculated with very low complexity, but they suffer from a high mean-square error [15]. MMSE channel estimation method estimate in terms of weight matrix. It employs the second-order statistics of the channel conditions to minimize the mean-square error [16]. Error value is calculated from channel vector in such a way that the MSE is minimized.

5.3.1 Least Square Channel Estimation

The principle of least squares is that the overall solution minimizes the sum of the squares of the errors made in solving every single equation. Compared to MMSE estimator LS estimator has lower computational complexity. It requires pilot symbols and matrix inversion. A training sequence is transmitted by each transmit antenna at the beginning of each data burst. The notation for transmitted signal is x , received signal is y , the column in F are orthogonal. The LS estimator for the cyclic impulse response g minimizes $(y - xFg)^H (y - xFg)$ and generates the channel attenuation as bellow

$$h_{LS} = F Q_{LS} F^H x^H y$$

$$\text{where } Q_{LS} = (F^H x^H F x)^{-1} \text{ and}$$

$$(y - xFg)^H \text{ are the conjugate transpose operations}$$

Matrix operation hermitian and inverse are commonly used in this method. The least square channel impulse response or channel attenuation is written as

$$h_{LS} = x^{-1}y$$

Hence, LS estimates are calculated without using any knowledge of statistics of the channel but they suffer from a high mean square error.

5.3.2 Minimum Mean Square Error Channel Estimation

The MMSE estimator major rule is to efficiently estimate the channel to minimize the MSE or symbol error rate (SER) of the channel by employing second-order statistics of the channel conditions. The constrain for MMSE channel estimation are auto-correlation matrix, auto-covariance matrix, noise variance. The notation for common signal are as follows, x is the transmitted signal, y is received signal, g_{MMSE} is the channel energy(impulse response of channel), h_{MMSE} is the channel attenuation (transfer function) for MMSE estimator and F is the DFT matrix.

The channel estimation by using MMSE estimator can be derived as follows:

$$g_{MMSE} = R_{gy} R_{yy}^{-1}y$$

$$\text{Where } R_{gy} = E\{gy^H\} = R_{gg}F^H x^H \text{ and}$$

$$R_{yy} = E\{yy^H\} = xFR_{gg}F^H x^H + (\delta_n)^2 I_n$$

Here the columns in F are orthogonal and I_n is the identity matrix of n^{th} order. The channel impulse response is as follows:

$$h_{MMSE} = F.g_{MMSE} = FQ_{MMSE}F^H x^H y$$

$$\text{where } Q_{MMSE} = R_{gg} [(F^H x^H x F) (\delta_n)^2 + R_{gg}]^{-1} (F^H x^H F x)^{-1}$$

Both estimators have their own drawbacks. However the LS estimator computational complexity is low, it has high mean-square error contrast to the MMSE estimator. Performance of estimator is tradeoff between the computational complexity and mean error. It is better to choose particular channel estimator base on requirement threshold and resource allocation.

5.4 Processing Domain Estimation

Channel estimation is classified in time and frequency domain based on which domain the estimator takes the received signal. In MIMO-OFDM system, IFFT converts the frequency domain message symbol in to time domain symbol and the time domain symbol is modulated via PSK/QAM modulation through AWGN channel [13].

5.5 Iteration versus Direct channel estimation

Based on the no of time the function execution, the estimator is classified in direct and iterative channel estimator. Direct channel estimation method solves the problem in one-shot while iterative method attempts to approach the exact solution of the system by finding successive approximations starting from an initial guess of channel information. Generally MIMO system use iterative approach to remove additive noise effects and achieve better performance. For small system with small no of variables, iterative methods are relative expensive than the direct ones.

5.6 DFT-Based Channel Estimation

The DFT-based channel estimation technique guided by the statement “the performance of LS or MMSE channel can be improved by eliminating the effect of noise outside the maximum channel delay”. Let $H[K]$ represent the estimate of channel gain at the K_{th} subcarrier, obtained by either LS or MMSE channel estimation method. Taking the IDFT of the channel estimate

$$IDFT \{H[K]\} = h[n] + z[n] \triangleq \hat{h}[n] \quad n=0, 1, \dots, N-1$$

where $z[n]$ the noise component in the time domain.

Ignoring the coefficients $h[n]$ that contain the noise only and defining the coefficients for the maximum channel delay L as

$$h_{DFT}[n] = \begin{cases} h[n] + z[n], & n = 0, 1, 2, \dots, L-1 \\ 0, & \text{otherwise} \end{cases}$$

and transform the remaining L elements back to the frequency domain as follows

$$H_{DFT}[K] = DFT \{h_{DFT}(n)\}$$

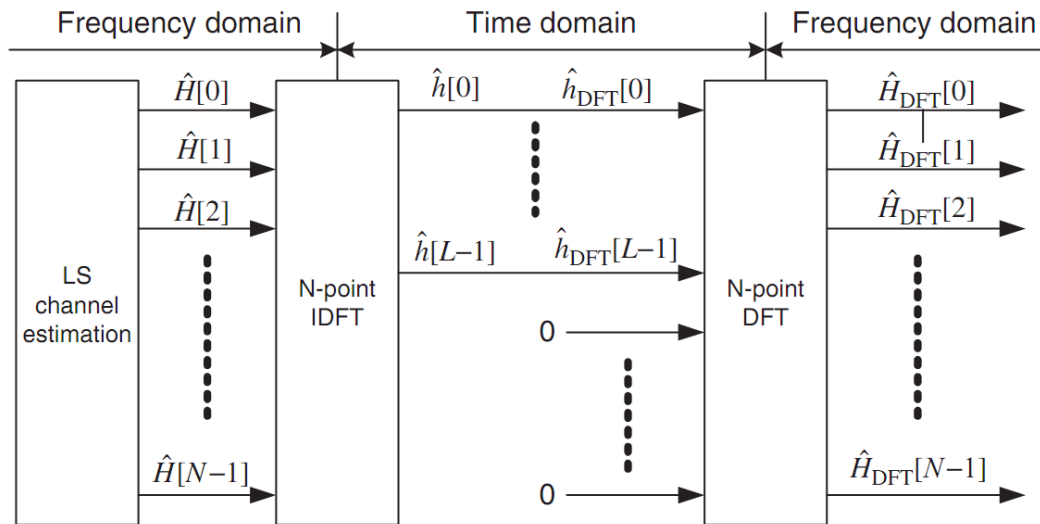


Fig 17 DFT-Based Channel Estimation

The block diagram of DFT-based channel estimation followed by LS channel estimation theory is shown in Fig17. The prerequisite condition for DFT-based channel estimation is the maximum channel delay L must be known in advance.

Rest of these techniques other more channel estimation technique is also developed with more advance logic. Decision Directed Channel Estimation technique use the preamble or pilot signal only during beginning of channel estimation after that the coefficients of channel can be updated with decision directed feedback loop to track the possibility of time varying channel.

5.7 Advanced Channel Estimation Technique

In advance channel estimation technique there are different methods based on characteristics of channel. Channel estimation using a superimposed signal estimate channel without losing the data rate but some portion of power allocated to training signal is wasted. The next one, Channel estimation in fast time-varying channel is more appropriate on stable channel characteristics within in OFDM symbol period. In fast time varying channel longer OFDM symbol period has serious effect on performance of channel estimation.

Another advance channel estimation technique is EM (Expectation-Maximization) algorithm based channel estimation. It is iterative channel estimation technique to find maximum likelihood detection [18]. This technique can be used when transmit symbol are not used so it is often called semi blind channel estimation. In Blind channel estimation technique the statistical properties of received signal is figured without restoring the preamble or pilot signal. Clearly this technique has advantage of excluding the overhead with training signals but needs a large no of received symbol to derive statistical properties.

5.7.1 Blind channel estimation technique

In a MIMO-OFDM system, coherent signal detection requires a reliable estimate of the channel impulse responses between the transmitting and receiving antennas. These channels can be estimated by sending training sequences. Furthermore, transmitting the training sequences is undesirable for some communication systems. Thus, blind

channel estimation for MIMO-OFDM systems has been an optimum solution for these difficulties [17].

Blind channel estimation scheme based on the noise sub space method unifies and generalizes MIMO-OFDM with any number of transmit and receive antennas. Furthermore, the proposed method achieves accurate channel estimation and fast convergence. In terms of both channel estimation accuracy and convergence speed, increasing the length of CPs rather than the number of VCs for the proposed method was found to improve the performance in the simulations significantly. In addition, by increasing an observed OFDM symbol block to an adequate dimension for channel estimation, it can achieve an accurate channel estimation in an MIMO-OFDM system with no or insufficient CPs, thereby potentially increasing channel utilization.

In this MIMO-OFDM system model with M_t is no of transmit side antennas and M_r is number of receive side antennas, as illustrated in Fig 18, show the baseband model of an OFDM system for the j^{th} transmit and i^{th} receive antennas which has N subcarriers and the uses subcarriers listed from (k_0) to $(k_0 + D - 1)$ for information data. The remaining $(N - D)$ unmodulated carriers are referred to as virtual carriers (VCs) that are needed for the input signal pulse shaping by the raised cosine filter (transmit filter) with a suitable roll-off factor. If D equal to N , the system no longer has VCs. Hence, this system model can be applied to both systems without and with VCs. Let the n^{th} block of the frequency-domain information symbols in the j^{th} transmit antenna be written as

$$d_j(n) = [d_j(n, k_0), d_j(n, k_0 + 1) \dots \dots \dots d_j(n, k_0 + D - 1)]^T \dots \dots \dots (1)$$

where j is the transmit antenna index with $1 \leq j \leq M_t$.

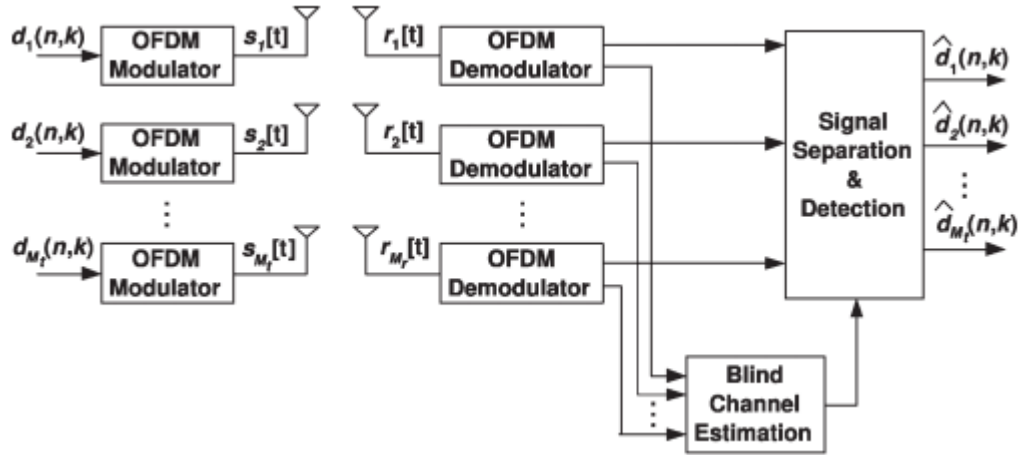


Fig 18 MIMO-OFDM system model with M_t transmit and M_r receive antennas

Suppose that the length of the cyclic prefix (CP) is P , each OFDM modulator adds $(N - D)$ zeros for VCs to the data block in equation (1), utilizes an N -point IFFT to this block, and inserts the CP in front of the IFFT output vector, which is a copy of the last P samples of the IFFT output. Such leaves in the time-domain sample vector of the n^{th} OFDM symbol written as

$$s_j(n) = [s_j(n, N - P), \dots, s_j(n, N - 1), s_j(n, 0), \dots, s_j(n, N - 1)]^T \dots \dots \dots (2)$$

Continuous-time signal is generated by pulse shaping the sample vector $s_j(n)$ with transmit filter $g_{tx}[t]$. And then sent through the channel, which is mathematically expressed as

$$s_j[t] = \sum_{n=-\infty}^{\infty} \sum_{k=0}^{Q-1} s_j(n, (N - P + k)N) g_{tx}[t - (k - nQ)T] \dots \dots \dots (3)$$

where $Q = N + P$, and T is the sample duration in the time domain.

By denoting $s_j(n, (N - P + k)N)$, meaning the k^{th} sample of the n^{th} OFDM symbol in the time domain, as $s_j((k + nQ)T)$, and $k + nQ$ as α , the transmitted signal $s_j[t]$ can be concisely expressed as

$$s_j[t] = \sum_{\alpha=-\infty}^{\infty} s_j(\alpha T) g_{tx}[t - \alpha T] \dots \dots \dots (4)$$

Then, M_t transmit antennas simultaneously transmit the signals $s_1[t], s_2[t], \dots, s_{M_t}[t]$.

Throughout the transmission period, the transmitted signal $s_j[t]$ from the j_{th} transmit antenna passes through a dispersive channel with an impulse response $c_{ij}[t]$. Spatially uncorrelated additive white Gaussian noise $v_i[t]$ corrupts the transmitted signal and corrupted signal enters into a front-end receive filter $g_{rx}[t]$ at the i_{th} receive antenna. When we denote the composite channel impulse response between the j_{th} transmit antenna and the i_{th} receive antenna as $h_{ij}[t] = g_{rx}[t] * c_{ij}[t] * g_{tx}[t]$, and the filtered noise at the i_{th} receive antenna as $\eta_i[t] = v_i[t] * g_{rx}[t]$, the received signal $r_i[t]$ at the i_{th} receive antenna is showed as

$$r_i[t] = \sum_{j=1}^{M_t} \sum_{a=-\infty}^{\infty} s_j(aT) h_{ij}[t - aT] + \eta_i[t] \dots \dots \dots (5)$$

Assume that the composite channel impulse responses $h_{ij}[t]$ have the finite support $[0, (L+1)T)$ with $L \leq P$, which ensure that $r_i[t]$ is not contaminated by former OFDM symbols. By sampling $r_i[t]$ at a rate $1/T_s = q/T$ with a positive integer q , the sampled received signal $r_i[iT_s + mTs] = r_i[iT + (mT/q)]$ at the i_{th} receive antenna is given as

$$r_i \left[\epsilon_i + \frac{mT}{q} \right] = \sum_{j=1}^{M_t} \sum_{l=0}^L s_j \left(\left[\frac{m}{q} \right] T - lT \right) \times h_{ij} \left[\epsilon_i + \frac{(m)qT}{q} + lT \right] + \eta_i \left[\epsilon_i + \frac{mT}{q} \right] \dots \dots (6)$$

where $\eta_i \in [0, Ts]$ is the sample timing error at the i_{th} receive antenna.

This is the basic model for channel estimation, based on varying no of antenna array in transmitter side and receiver side it can be categorized in different sub model. In this thesis work the normalized root mean square error (NRMSE) performance of channel is compared with different value of SNR and no of OFDM symbols.

6 Simulation and Result

In the thesis there are all together eight simulations are done to evaluating the performance of MIMO OFDM system. First four are concerning with PAPR reduction and later remaining are for channel estimation. The effects of OFDM signal and no of subcarrier on PAPR characteristics in SLM method are shown in first simulation. In next simulation the effects of subblock partition and different value of phase factors on PAPR characteristics in PTS method are presented. Third simulation compares the PAPR characteristics between SLM and PTS technique. OFDM system can be make equivalent to single carrier system by implementing same size of IFFT as a spreading code. Subcarrier assigning can be done in different approach so performance of PAPR due to DFDMA, LFDMA and IFDMA subcarrier assignment is compared in different modulation scheme. Results of pulse shaping and subcarrier variation in DFT-spreading method are also analyzed in the simulation. BER in Alamouti space time block code with different number of transmitter antenna and receiver antenna are sketched in fifth simulation. Sixth simulation evaluates the MSE & SER of LS and MMSE channel estimator. Next preceding simulation compares the DFT-based channel estimation performance with conventional LS and MMSE channel estimator. Finally the NRMSE simulation of Blind channel estimation is carried out.

6.1 PAPR characteristics in SLM

Here simulation with different values of route number (M) or OFDM signal no and no of subcarrier (N) is conducted, and the results exhibits some desired properties of signals representing the same information. In simulation rotation factor is defined as $P_{m,n} \in [\pm 1, \pm j]$, iteration time for algorithm is 10000 times, oversampling factor is 8 and QPSK is adapted to subcarrier.

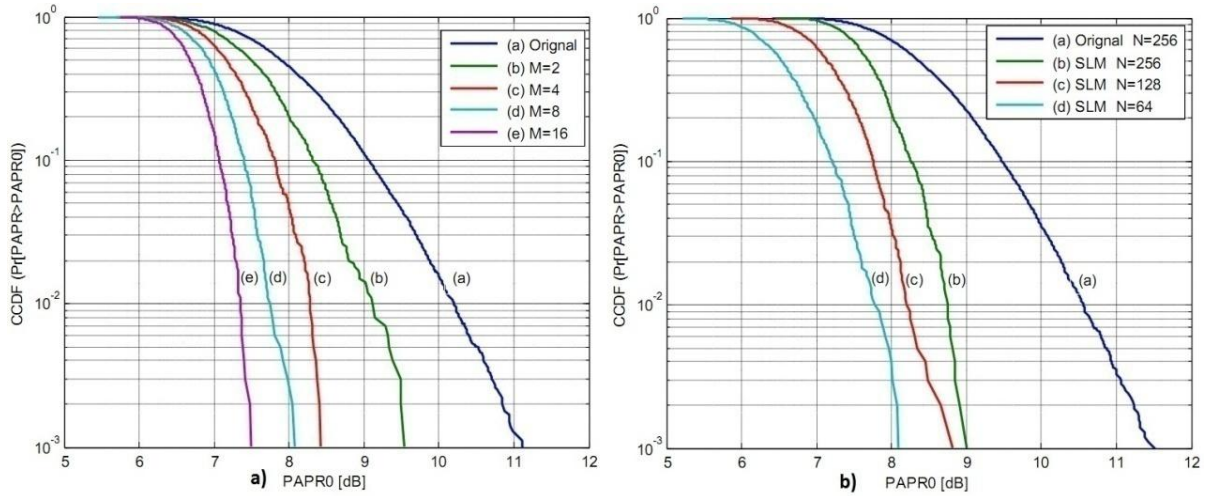


Fig 19 PAPR reduction performances with a) different values of route number with subcarrier $N=128$ b) different values of subcarrier with route number $M=8$

It can be observed that the proposed SLM method displays a better PAPR reduction performance than the original OFDM signal which is free of any PAPR reduction scheme. The following statement can be stated after the analysis of above simulation based on Fig 19.

- SLM method can significantly amend the PAPR distribution of OFDM system i.e. significantly cut down the presenting probability of large peak power signal. To get small improvement of PAPR reduction performance by increasing OFDM signal number M , we have to pay high complexity. These problems pose a very high charge on real OFDM implementation; so to reduce the computational complexity in practical application, compromise the computing complexity and improvement of performance, it is better to take $M \leq 8$.
- Since SLM algorithm can be used for different OFDM systems with different number of carriers, it is more appropriate for the OFDM system with a large number of sub-carriers (more than 128).

6.2 PAPR characteristics in PTS

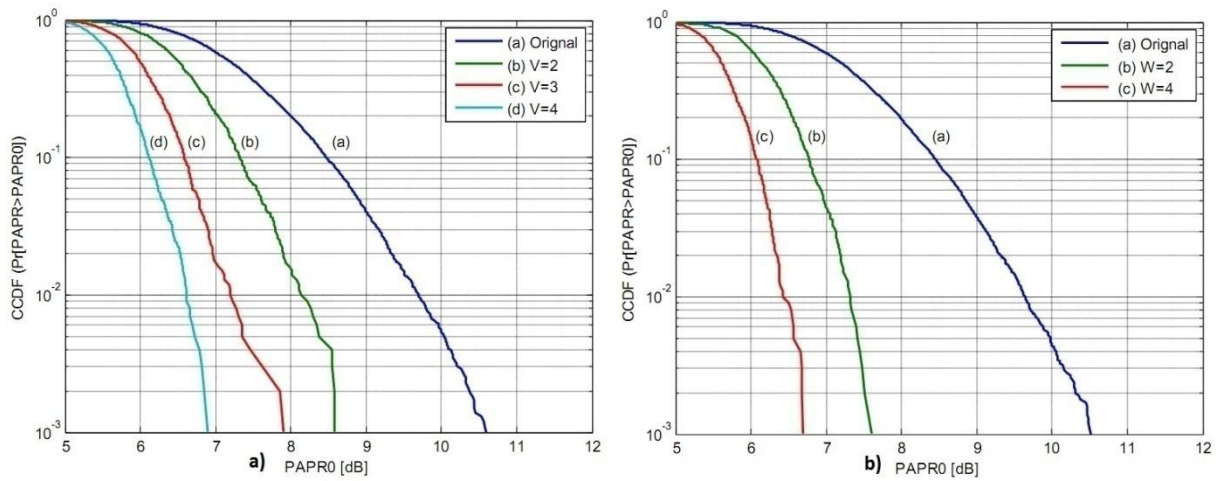


Fig 20 PAPR reduction performances with a) different values of no of subblocks V b) different values of no of allowed phase factors W

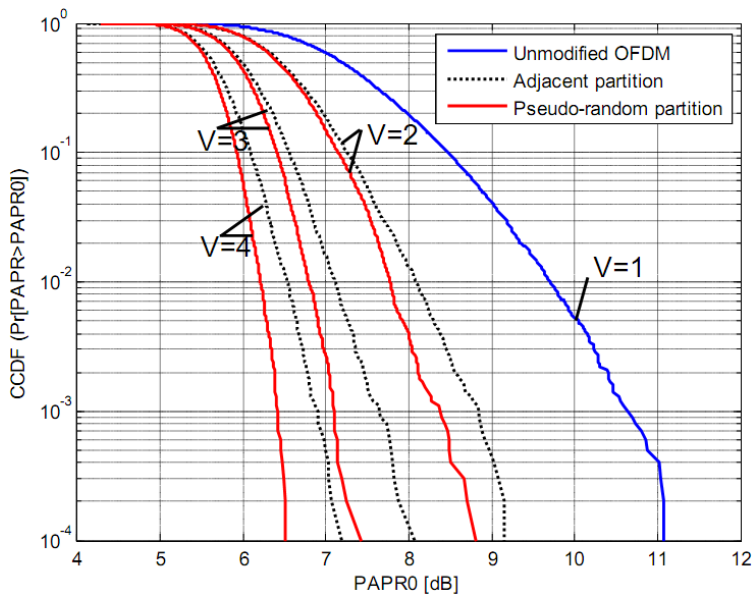


Fig 21 PAPR reduction performances with different subblocks partition schemes

It can be observed that the proposed PTS method displays a better PAPR reduction performance than the original OFDM signal which is free of any PAPR reduction scheme. The following statement can be stated after the analysis of above simulation with QPSK modulation, number of subcarrier ($N=256$) and oversampling factor ($L=8$).

- From the Fig 20(a), the performance of OFDM system increasing with higher no of sub-blocks. lets set the probability of PAPR at 1% the CCDF curve at different value of V , it is observed that 3dB improvement when $V=4$ and 1.5 dB improvement when $V=2$ than that of conventional OFDM.
- From the Fig 20(b), the performance of OFDM system increasing with more the number of the allowed phase factors. lets set the probability of PAPR at 1% the CCDF curve at different values of no of allowed phase factors W , it is observed that around 3dB improvement when $W=4$ and 1.5 dB improvement when $W=2$ than that of conventional OFDM
- From the Fig 21, the performance of OFDM system increasing with sub-block partition schemes. Among these, the pseudo-random partition scheme has better performance in all value of V .

6.3 Comparison between SLM and PTS algorithm

6.3.1 Auxiliary information comparison

SLM and PTS algorithms are two typical signal scrambling techniques for reducing PAPR in OFDM system. In order that have error-free demodulation in the receiving end, side information must be sent to the receiver, in accurate manner. Hence, in practical application often requires the use of some coding measures to ensure reliability of information from being disturbed. Since this comparison only concentrates on studying PAPR reduction performance in MIMO-OFDM system with different algorithms, and does not reflect on the modulation in receiving end. Thus, it expresses at the redundancy of subsidiary information rather than coding redundancy.

For the notation of collection range of weighting factor W , then for sub-blocks V , the system exists W^{V-1} types of auxiliary information sequence, so the number of redundant bits is $R_{ap} = (V-1) \log_2 W$. Like in same manner in SLM method, if the length of sequence P_m is M , then in SLM-OFDM system, it requires redundant bits $R_{ap} = \log_2(M-1)$. As can be seen from Table 2 below, in same situation, SLM method requires a lower information redundancy, compare to PTS algorithm.

Table 2 SLM and PTS Comparison with different M V values

Scrambling Technique		Partition number	M=V=2	M=V=4	M=V=8	M=V=16
SLM			0	1.58	2.81	3.91
PTS	W=2		1	3	7	15
	W=4		2	6	14	30
	W=6		3	9	21	45

6.3.2 Comparison of PAPR reduction performance between SLM and PTS

Fig. 22 shows the simulation result of using SLM and PTS method to an OFDM system, individually. In PTS method, we fix the number of sub-carriers $N = 128$ and applying pseudo-random partition scheme, for each carrier, adopting QPSK constellation mapping, weighting factor $b_v \in [\pm 1, \pm j]$; In SLM method, rotation factor $P_{m,n} \in [\pm 1, \pm j]$. On the basis of theory, we know that the IFFT calculation amount of these two methods is same when $V = M$, but for PTS method, it can provide more signal manifestations, thus, PTS method should provide a better performance on PAPR reduction. In fact, this deduction is confirmed by simulation result. From the Figure 22, it can be learned that with the same CCDF probability 1%, the PAPR value equals to 7dB when PTS is employed, while the PAPR raise up to 8.2dB when SLM is employed under the same consideration.

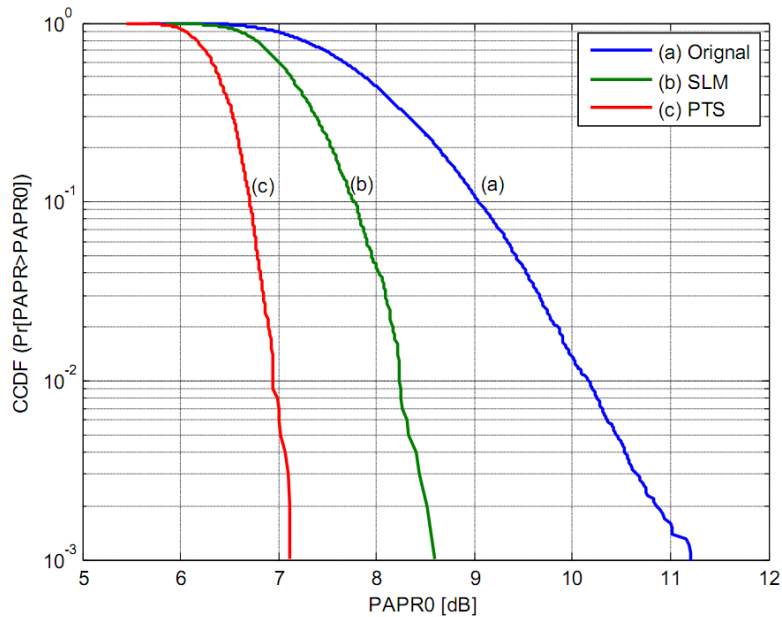


Fig 22 Comparison of PAPR reduction performances between PTS algorithm and SLM algorithm for MIMO-OFDM system

On the basis of Fig 22, it can be said that PTS technique provides a better PAPR reduction performance compared to SLM technique. However, the cost is also compensated for sacrificing transmission efficiency and rising complexity. Therefore in real implementation scenario, a tradeoff should be made between good performance and auxiliary information. Regarding the above discussion, it can be said that SLM algorithm is more suitable if system can tolerate more redundant information, elsewhere, PTS algorithm is more favorable when complexity does not become the prime considering factor. In brief, compromise will be made for a reliable system.

6.4 PAPR characteristic in DFT-spreading technique

To illustrate the appraisal of DFT-spreading technique, simulation is done by taking different modulation schemes such as QPSK, 16-QAM, and 64-QAM. PAPR performances due to DFT-spreading technique on the IFDMA, LFDMA, and OFDMA sub-carrier assigning approaches are compared in all above modulation schemes. From

this plot (Fig 23 it can be said that interleaved FDMA has the best PAPR reduction performance among other subcarrier assigning approach.

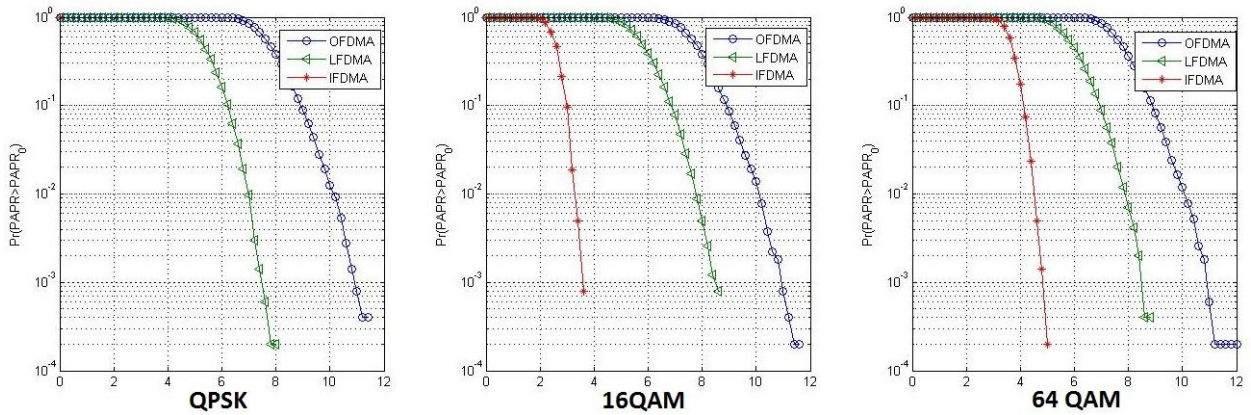


Fig 23 PAPR performances of DFT-spreading technique for IFDMA, LFDMA, and OFDMA

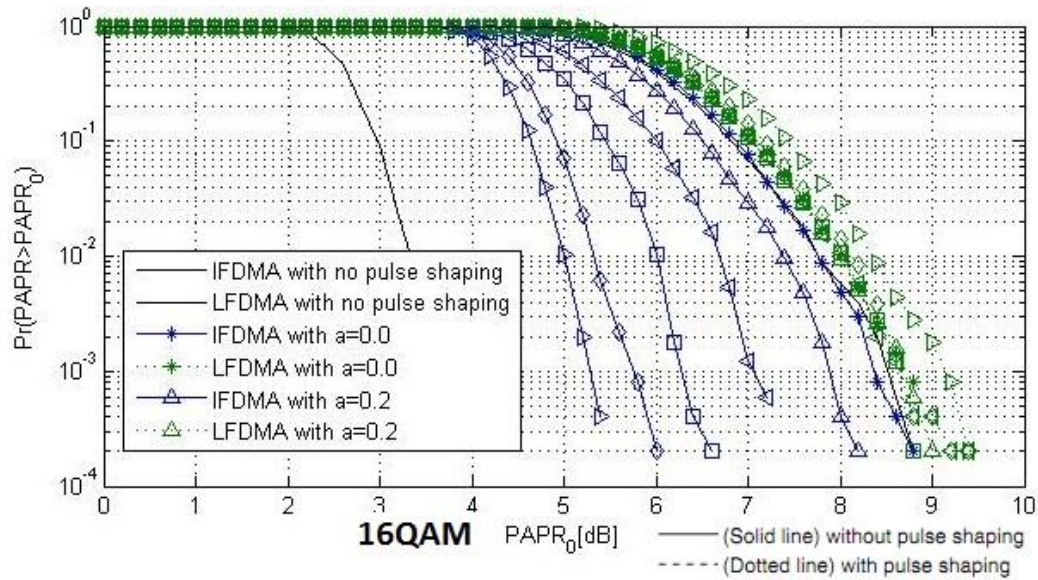


Fig 24 PAPR performances of DFT-spreading technique with pulse shaping

Pulse shaping is the process of changing the waveform of transmitted pulses to make the transmitted signal better suited for communication channel by limiting the effective bandwidth of the transmission. Raised-Cosine filter is popular in wireless communication. It can be seen from Fig 24 that the PAPR performance of IFDMA can

be significantly improved by increasing the roll-off factor from 0 to 1. This is in contrast with LFDMA which is not so much affected by pulse shaping. This means IFDMA will have a trade-off between excess bandwidth and PAPR performance since excess bandwidth decreases as the roll-off factor becomes smaller.

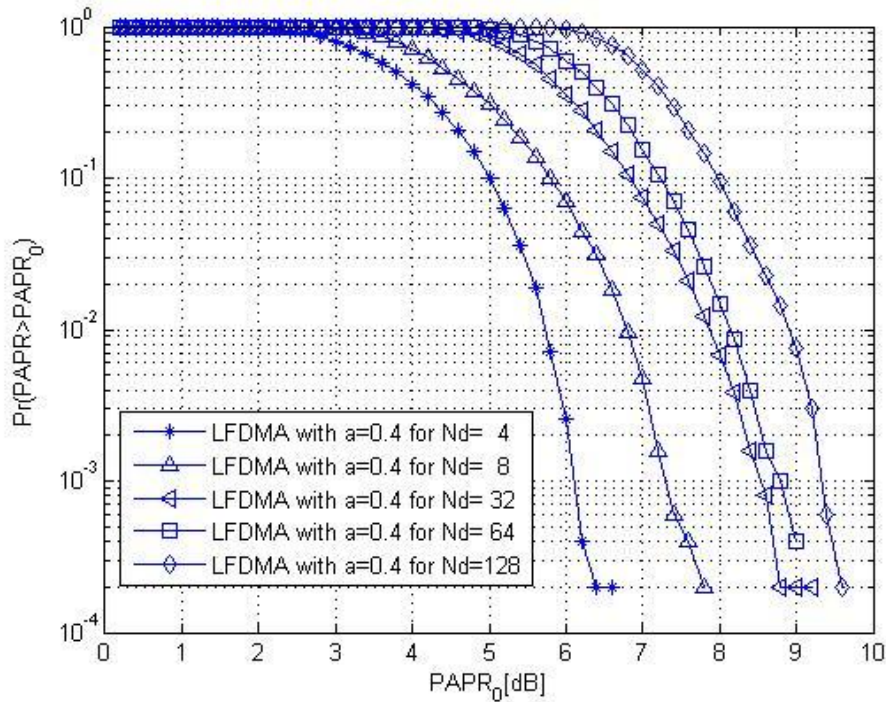


Fig 25 PAPR performance of DFT-spreading for variable subcarrier

To see the dependency of the number of subcarriers in PAPR performance of DFT-spreading technique for LFDMA, simulation of CCDF versus PAPR is plotted. The simulation parameter are roll-off factor of a 0.4, modulation 64-QAM and SC-FDMA system with 256-point FFT.

Finally it can be said from above experiment that, the SC-FDMA systems with IFDMA and LFDMA have a better PAPR performance than OFDMA systems. In spite of, the IFDMA has a lower PAPR than LFDMA, the LFDMA is usually opted

for implementation because, subcarriers allocation with equi-distance over the entire band is quite difficult to implement, since OFDMA requires additional resources such as guard band and pilots.

All PAPR reduction techniques have their own advantages. Nevertheless even a single method is the perfect one for PAPR problem. The judgment of particular method is based on requirement. It is better to choose the particular method by keeping in mind following parameters such as transmit power signal level, BER at receiver, loss in data rate, computational complexity etc

6.5 Bit Error Rate in MIMO

Bit error rate (BER) in Alamouti space time block code with different number of transmitter antenna and receiver antenna are sketched. The simulation is done by taking 10^6 no of BPSK symbol and SNR values is taken upto 25 dB.

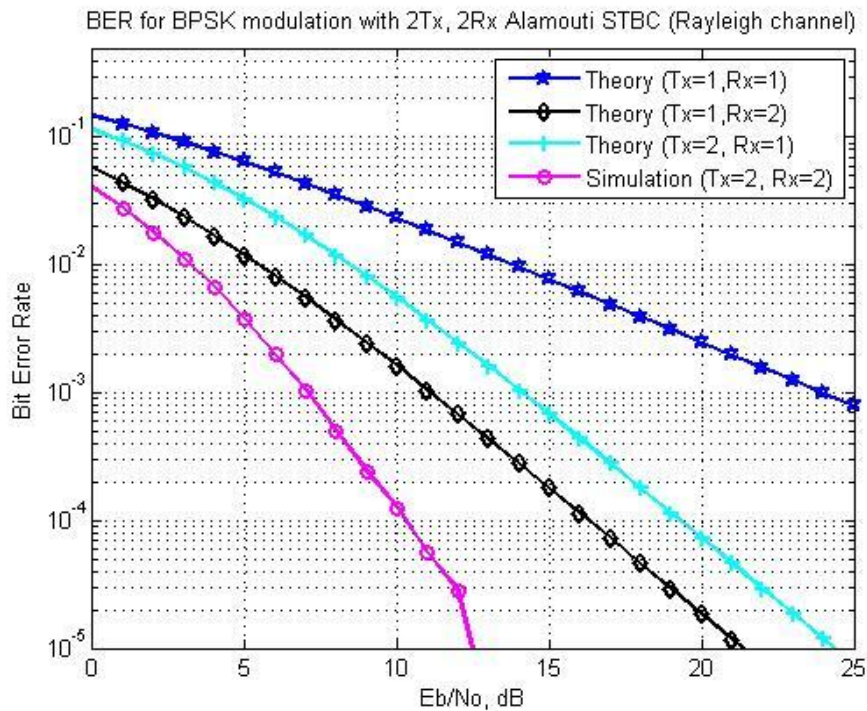


Fig 26 Bit error rate for various antenna arrangements

On the basis of; theoretical calculation and simulation in MATLAB; SISO configuration has the worst BER performance among all other configuration. MIMO with two transmitters and two receivers has least bit error rate for BPSK modulation. Furthermore based on the Fig 26 BER performance of single transmitter with two receivers has 3 dB better performances than two transmitters with one receiver configuration.

6.6 Comparison of LS and MMSE Estimator

The simulation consists of two important parameter, called mean square error (MSE) and symbol error rate (SER), comparisons between LS and MMSE estimator with two main programs. The MSE of an estimator measures the difference between the true value of the quantity being estimated and the theoretical values of an estimator. MSE evaluates the average of the square of the error. MSE is defined as

$$\text{Mean square error} = \text{mean} [\{ \text{abs}(H) - \text{abs}(h_{\text{estimator}}) \}^2]$$

Where, H is theoretical transfer function and

$h_{\text{estimator}}$ is the calculated transfer function for each estimator.

Number of symbol changes made to the transmission medium per second using a digitally modulated signal is called SER. Symbol error rate for 16-QAM system is

$$P_{SER-QAM} = 3/2 \operatorname{erfc} \left(\sqrt{\frac{E_s}{10 N_0}} \right)$$

where, erfc denoted complementary error function,

E_s denoted signal energy and

N_0 denoted bit rate

The LS estimation, Frequency response from LS estimator is calculated by using input signal and theoretical value of signal. The impulse response of the LS estimator is calculated from MATLAB and used for calculation of mean square error.

In MMSE estimation, Auto-correlation function of channel energy, Auto-correlation function of output signal and Cross-correlation of the channel energy and output signal is calculated by using the MATLAB simulator. By using these values, impulse response function and the transfer function of estimator are calculated and finally using these function mean square error and symbol error rate is calculated.

The attribute used for simulation are FFT size 64, Number of sub-carrier 64, pilot ratio 1:10, guard length 10, guard type is cyclic prefix, bandwidth is 500 KHz and modulation scheme is 16-Quadrature Amplitude Modulation (QAM).

Table 3 LS and MMSE comparison

	The MMSE estimator	The LS estimator
The given inputs signal	x	x
Theoretical frequency response	H	H
The output signal	y	y
The channel energy	g	
Auto-correlation function of channel energy	R_{gg}	
Cross-correlation function of the channel energy and output signal	R_{gy}	
Auto-correlation function of output signal	R_{yy}	
Noise variance $E\{ n ^2\}$	$(\delta_n)^2$	

In this simulation, the channel estimation based on time domain channel statistics is described. Using a general model for a slowly fading AWGN channel, we present the MMSE and LS estimators. The MSE and SER for a BPSK system is demonstrated by means of simulation. Depending upon estimator complexity in MSE performance, up to 4 dB in SNR can be gained in MMSE estimator over the LS estimator in 1% probability of error. In SER simulation both estimator have nearly same characteristics.

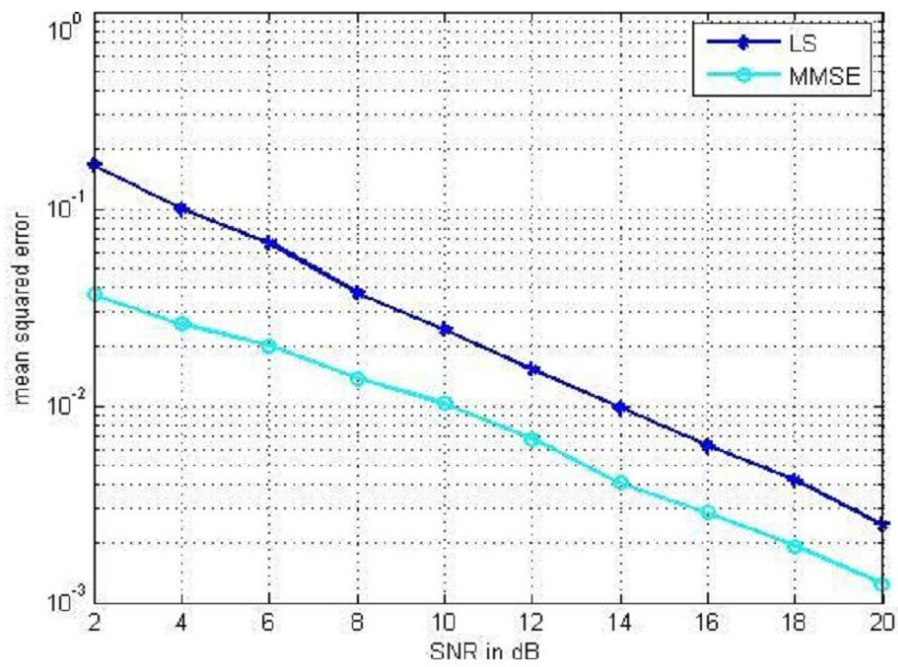


Fig 27 Mean Square Error comparison for LS and MMSE estimator

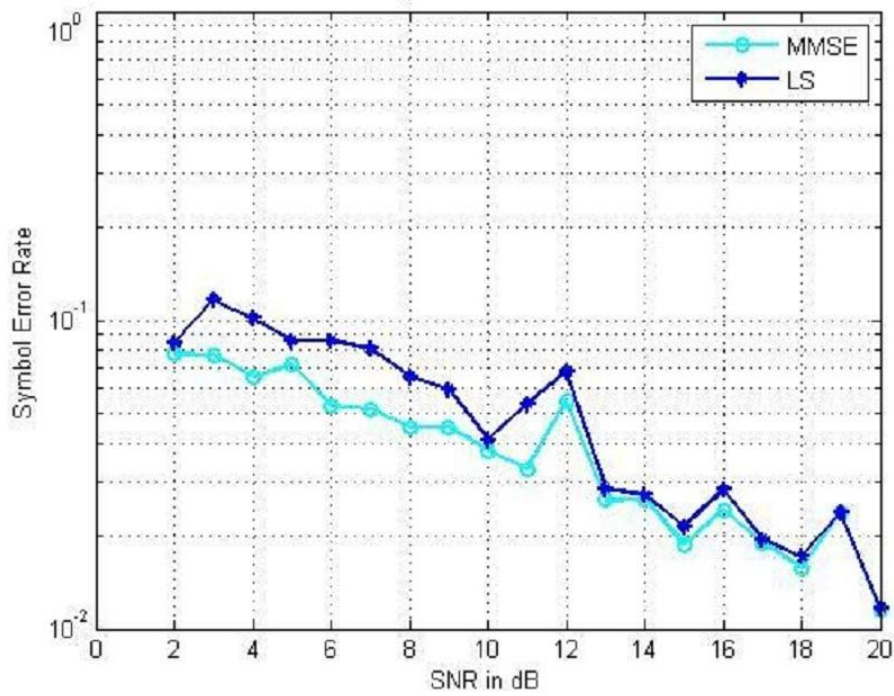


Fig 28 Symbol Error Rate comparison for LS and MMSE estimator

6.7 DFT Based Channel Estimation

Figure 29 show illustrating the effect of channel estimation by plotting the received signal constellation before and after channel compensation for the OFDM system with 16-QAM. In the same manner Fig 30 illustrates the channel estimates obtained by using the various types of channel estimation methods with and without DFT technique.

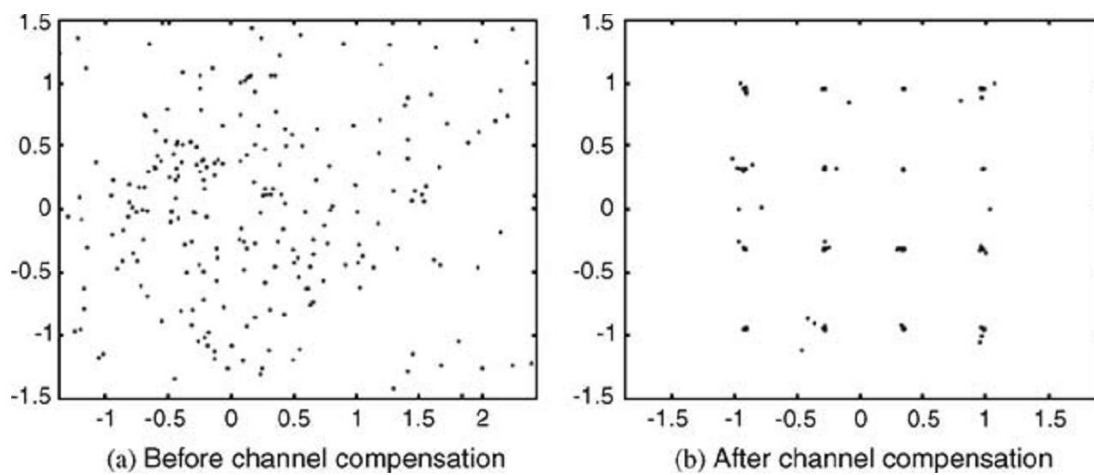


Fig 29 Constellation diagram of received signal

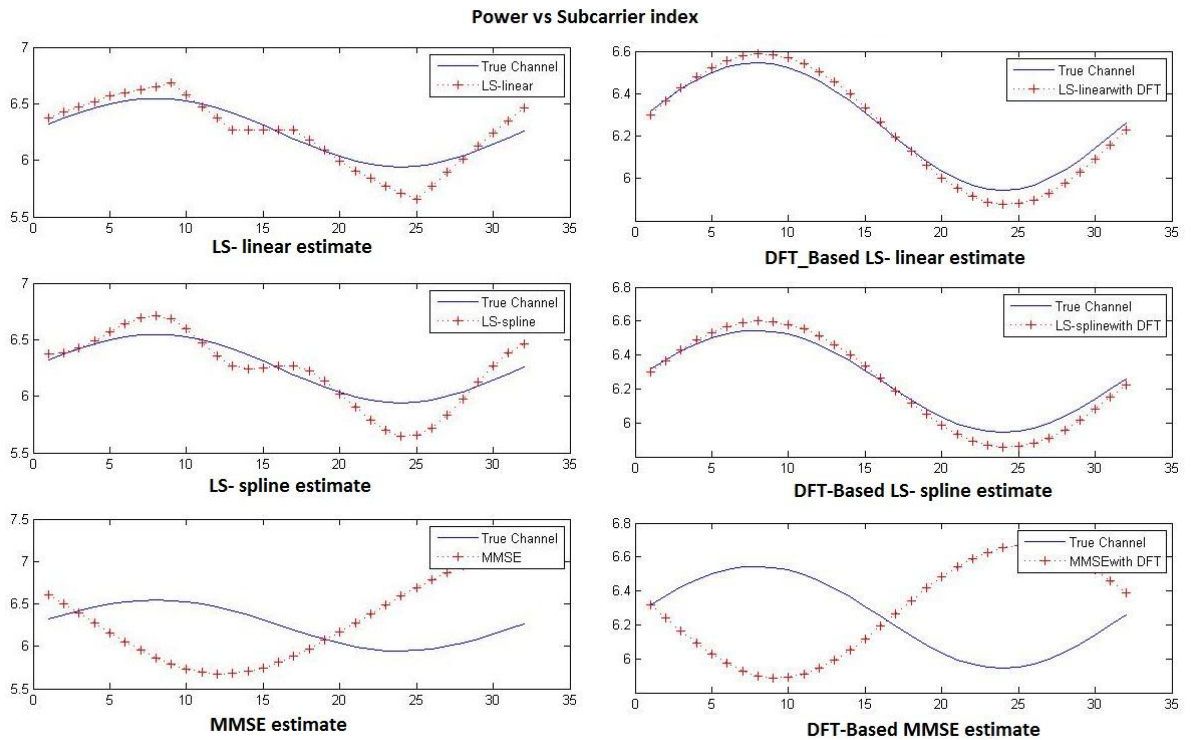


Fig 30 Comparison with and without DFT-Based channel estimation

Based on the simulation of DFT-Based channel estimator on LS- linear, LS-spline and MMSE estimation all three shows the better performance than DFT not used channel estimator. Channels are generated by using Gaussian random number function “randn.” It is also seen that MMSE estimator has better performance than LS estimator at the trade of requirement of additional computing and channel characteristics information.

6.8 NRMSE simulation for blind channel estimation

To evaluate the performance of the blind channel estimation method, assuming MIMO-OFDM system with two transmits antennas and two receive antennas. The number of subcarriers is assign to 64. Information symbols are independent and identically distributed 16-QAM symbols. Channel is time-invariant during each channel estimation and additive noise at each receive antenna is a spatially uncorrelated complex white Gaussian noise with zero mean and σ^2 variance. The order of the MIMO channel is considered to be $L = 3$. The transmit power per OFDM symbol is defined to E_s . The SNR of this channel is written as

$$SNR \triangleq 10 \text{Log}_{10} \frac{M_t(L+1)\sigma_h^2 E_s}{(N+P_0)\sigma_\eta^2} \text{ (dB)}$$

Where P_0 is the maximum value of cyclic prefix

To measure the performance of channel estimation we have to calculate normalize root mean square error of system which is given as

$$NRMSE = \sqrt{\frac{1}{N_m M_t M_r (L + 1)} \sum_{k=1}^{N_m} \sum_{i=1}^{M_t} \frac{\|h_i^{(k)} - \hat{h}_i^{(k)}\|_2^2}{\|h_i^{(k)}\|_2^2}}$$

Where N_m is the no of Monte Carlo trials, the subscript k signifies the k_{th} Monte Carlo trial $h_i^{(k)}$ and $\hat{h}_i^{(k)}$ represents true channel response vectors and estimated channel response vectors respectively. NRMSE provides a measure of how well the true MIMO channel and the estimated MIMO channel by the blind channel estimation method span the same M_t -dimensional space.

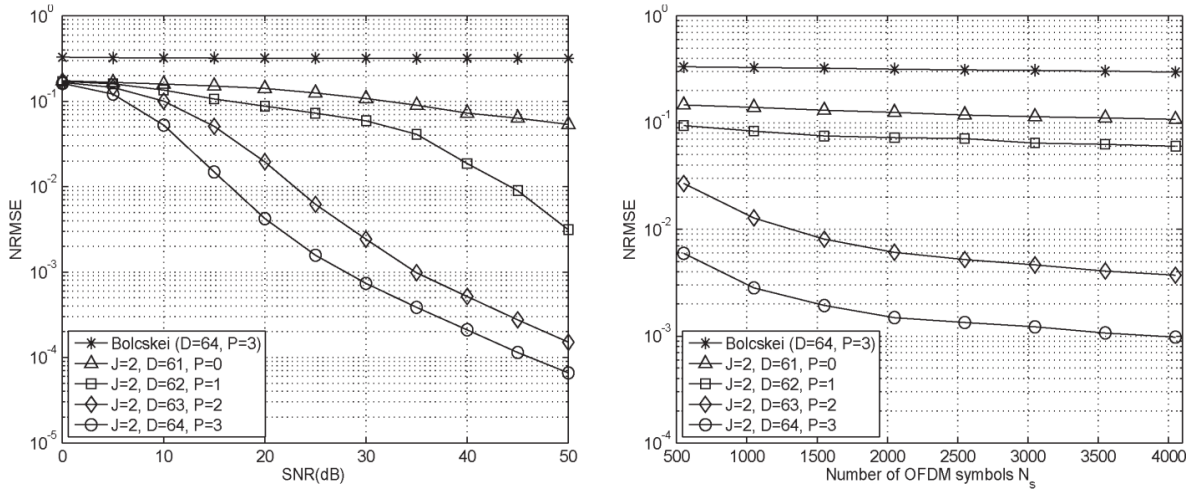


Fig 31 Comparison of NRMSE performance vs SNR (left) and no of OFDM symbols (right)

Regarding the Fig 31, it is clear that for fixed value of no of OFDM symbol is fixed to 2000, NRMSE decrease with the increase in SNR. Moreover cyclic prefix is also performance determining factor and increasing its no gradually decrease the error probability. Right side of Fig 31 shows the NRMSE versus no of OFDM symbols for fixed value of SNR (25 dB). Here also NRMSE is inversely proportional to number of OFDM symbol and by same way higher the no of cyclic prefix, better the error performance.

7 Conclusions and Future works

7.1 Conclusions

On the basis of above eight simulations some remarkable decision are delivered on the performance evaluation of MIMO OFDM system. To get small improvement of PAPR reduction by increasing OFDM signal number, we have to pay high complexity in SLM technique. Furthermore, it is better for the OFDM system with a large number of sub-carriers. In PTS technique at 1% probability of error with four numbers of subblocks and allowed phase factors has around 3dB improvement than that of conventional OFDM. Moreover, PAPR performance of OFDM system increases with sub-block partition schemes. Based on the Comparison of PAPR reduction performances between PTS algorithm and SLM algorithm, PTS technique provides a better PAPR reduction performance compared to SLM technique in trade-off for sacrificing transmission efficiency and rising complexity. From the simulation of PAPR characteristic in DFT-spreading technique with different approach of subcarrier assignment policy interleaved FDMA has the best PAPR reduction performance. Even more pulse shaping with higher roll-off factor has better performance. All PAPR reduction techniques have their own features. Nevertheless even a single method is the perfect one for PAPR problem. The judgment of choosing the particular PAPR reduction method based on transmit power signal level, BER at receiver, loss in data rate and computational complexity be the better criteria of selection.

In MIMO system with Alamouti space time block code, one transmitting antennas with two receiving antennas system has 3 dB better performances than two transmitting antennas with single receiving antennas system configuration at 0.1% BER. From the comparison of channel estimation technique between LS and MMSE, MSE performance of MMSE estimator has 4 dB in SNR can be gained in 1%

probability of error. From the simulation of DFT-Base channel estimation technique the statement “the performance of LS or MMSE channel can be improved by eliminating the effect of noise outside the maximum channel delay” is verified and all three channel estimator LS- linear, LS-spline and MMSE estimation show the better performance after DFT-Based channel estimation. In blind channel estimator for both variable SNR and OFDM symbol cases NRMSE decrease with increasing SNR and OFDM symbol record length N_s . Furthermore, the proposed method demonstrates much better bandwidth optimization performance than the training based channel estimation method.

7.2 Future works

Future wireless communication systems are supposed to deliver better QoS, wide coverage and higher data rate; In spite of those features they should be power and bandwidth efficient and should be capable of being deployed in highly dispersive wireless environments. On the other hand, the nature of wireless system is non-deterministic and it gets varied in short duration. Channel modeling based on considering geographical topology, climate characteristics and nature of scatters give better design. This thesis mainly focused on enhancing the performance of MIMO-OFDM wireless communication system. The combination of Linear Precoding & Blind Channel Estimation in MIMO, OFDM wireless communication system adaptive power transmit at receiver, extend the received signal strength at receiver and significantly reduce the length cyclic prefix.

MIMO-OFDM system has lots of topic like spectral efficiency utilization, power optimization, channel estimation, equalization and detection, minimizing BER etc. Enhancing information throughput maintaining high reliability is one of the emerging topics in this system. Finding out best combination of diversity, coding, channel estimation techniques, combining techniques and equalization techniques for different channel conditions is always an open research question in this field.

Reference:

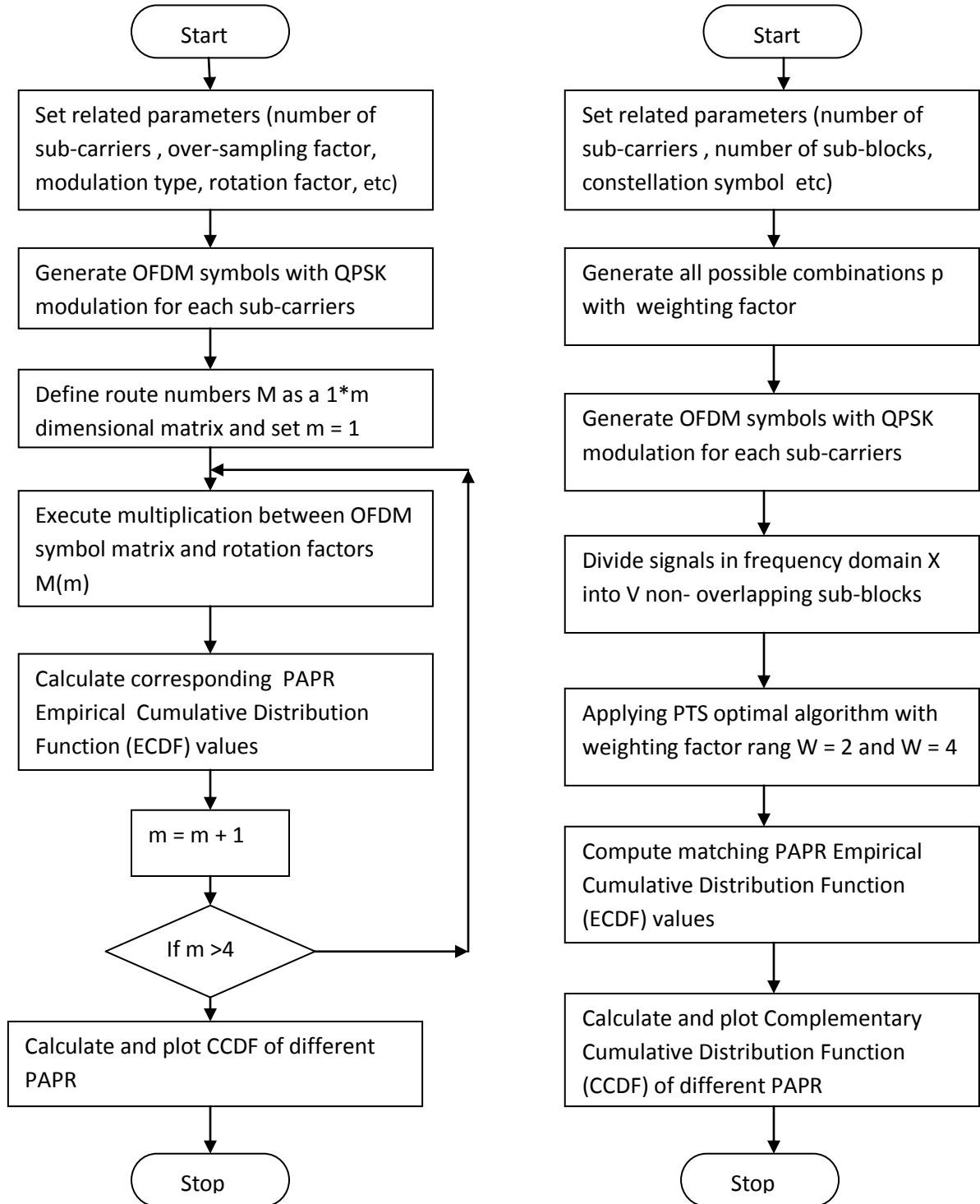
1. Ming Jiang; Hanzo, L, "Multiuser MIMO-OFDM for Next-Generation Wireless Systems", Proceedings of the IEEE, Vol. 95, Pp. 1430 – 1469, July 2007.
2. Stuber, G.L.; Barry, J.R.; McLaughlin, S.W.; Ye Li; Ingram, M.A.; Pratt, T.G.; "Broadband MIMO-OFDM Wireless Communications", Proceedings of the IEEE, Vol. 92, No. 2, Feb 2004.
3. Rony Kowalski "The Benefits High Dynamic Adaptive Modulation for High Capacity of Wireless Backhaul Solutions", Ceragon Networks, October 2007.
4. Ashish Pandharipande, "Principles of OFDM", IEEE Potentials 2002
5. Yan Xin, Georgios B. Giannakis, "High Rate Space Time Layered OFDM", IEEE Communications letters, Vol. 6, May 2002
6. Weinstein, S. B., and P.M. Ebert, "Data Transmission by Frequency Division Multiplexing Using the Discrete Fourier Transform," IEEE Trans. Communications, Vol. 19, pp. 628–634, Oct 1971, pp. 628–634
7. S. Alamouti, "A simple transmit diversity technique for wireless communications," IEEE J. Select. Areas Commun., vol. 16, pp. 1451–1458, Oct. 1998.
8. V. Tarokh, H. Jafarkhani, and A. R. Calderbank, "Space–time block codes from orthogonal designs," IEEE Trans. Inform. Theory, vol.45, pp. 1456–1467, July 1999.
9. V. Tarokh, N. Seshadri, and A. R. Calderbank, "Space–time codes for high data rate wireless communication: Performance criterion and code construction," IEEE Trans. Inform. Theory, vol. 44, pp. 744–765, Mar. 1998.
10. P.W. Wolniansky, G. J. Foschini, G. D. Golden, and R. A. Valenzuela, "V-Blast: An architecture for realizing very high data rates over the rich-scattering channel," in Proc. Int. Symp. Signals, Systems and Electronics (ISSE 1998), pp. 295–300.

11. Rick S. Blum, Ye (Geoffrey) Li , Jack H. Winters and Qing Yan, “ Improved Space Time Coding for MIMO-OFDM Wireless Communication”, IEEE Transactions on Communications, Vol. 49, Nov 2001.
12. Ramjee Prasad “ OFDM for Wireless Communication System” Universal personal communication, 2004
13. Yong Soo Cho, Jaekwon Kim, Won Young Yang, Chung G. Kang, " MIMO-OFDM Wireless Communications with MATLAB", John Wiley & Sons (Asia) Pte Ltd
14. Ana Aguiar, James Gross, "Wireless Channel Models", Technical University Berlin, Telecommunication Networks Group, April 2003
15. Markku Pukkila (Nokia Research Center), “Channel Estimation Modeling” Helsinki University of technology, S-72.333 Postgraduate Course in Radio communications.
16. Yushi Shen and Ed Martinez, “Channel Estimation in OFDM Systems” Freescale Semiconductor Application Note, Rev 0, 1/2006
17. Changyong Shin, Robert W. Heath, Edward J. Powers, “Blind Channel Estimation for MIMO-OFDM Systems”, IEEE Transactions on Vehicular Technology, Vol. 56, No. 2, March 2007.
18. Kang Zheng, Feng Tian, Guowen Huang and Min Bei “Unified ML channel estimator for MIMO-OFDM systems with virtual carriers” IEEE International Conference on Communication Technology (ICCT), pp. 409 – 412, Nov. 2010
19. Hassen Karaa, Raviraj S. Adve and Adam J. Tenenbaum, “Linear Precoding for Multiuser MIMO-OFDM Systems”, IEEE International Conference on Communications, Pp. 2797 – 2802, Aug 2007.
20. T. S. Rappaport, “Wireless Communications, Principles and Practice”, New Jersey: Prentice-Hall, 1996
21. Jeon, W.G., Chang, K.H., and Cho, Y.S. “An adaptive data predistorter for compensation of nonlinear distortion in OFDM systems”. IEEE Transactions on Communications, Vol. 45, No. 10, Oct 1997.
22. Antonio F, Hamdy W, Heidmann P, Heizer J, Kasturi N, Osés D P, Riddle C; " A novel adaptive predistortion technique for power amplifiers"; Vehicular Technology Conference 1999 IEEE 49th, Jul 1999

23. S. H. Muller, J. B. Huber, "A novel peak power reduction scheme for OFDM," The 8th IEEE International Symposium on Personal, Indoor and Mobile Radio Communications, Feb 1997
24. A. Katalinic, R. Nagy, and R. Zentner, "Benefits of mimo systems in practice: Increased capacity, reliability and spectrum efficiency," 48th International Symposium ELMAR-2006 focused on Multimedia Signal Processing and Communications, June 2006.

Appendices

1 Flow chart of SLM (left) and PTS (right)



Flow chart of procedure used in comparison of PAPR reduction performance with Selected Mapping (left) with different values of OFDM signal number (M) while sub-carrier number (N) is fixed at 128 and Partial Transmit Sequence (right) with different value range phase factor (W)

2 PAPR reduction comparison between SLM and PTS method

